STUDIES OF THE CHARACTERISTIC BEHAVIORS OF SPONGE-IRONS AND REDUCED PELLETS

MICHIO INOUYE and YOSHIAKI IGUCHI

Department of Metallurgy

(Received November 7, 1972)

CONTENTS

General Introduction

The direct reduction processes of iron ores have been the important subjects in the iron and steel industry for a long time. Now-a-days, they are developed to several practices only for the special purposes, because of the inferiority of producibility and also the economic disadvantage compared with the blast furnace practice.

Recently, the blast furnace practice have been improved remarkably beginning with the early use of self-fluxed sinter burdens, followed by low slag volume pellet burdens, and such advancements in operating techniques as controlled blast moisture, auxiliary fuel injection, and higher blast temperature. The further improvement of the blast furnace operations would be attained with prereduced pellet burdens.

On the other hand, it is to be noted that a shortage of the high quality coking coals for the blast furnace is a difficult problem for the increasing production of steel.

From the point of view mentioned above, the direct reduction methods would become more important in the future.

The most remarkable problem is the so-called iron and steelmaking process by the application of atomic energy. Although there are some difficult problems for this process, it is now considered that the direct reduction method will be most advantage combining with electric furnace steelmaking for the application

of neuclear energy.

However, one of the difficulties of the direct reduction process is the prevention of reoxidation of reduced iron even if the lump ores or pellets are used.

The purpose of the present work is to clarify the characteristics of the reduced iron or so-called sponge iron produced from various kinds of iron ores. Furthermore, as the anti-activation of such reduced iron is desired for the practical processes, so the present work was also undertaken for the useful method of the antiactivation.

Chapter I. Reoxidation Behaviors of Sponge-Irons Reduced from Ferric Oxide and Iron Ores

1.1. Introduction

It is well known that the reduced iron is active. But it has been little known on the characteristics of sponge irons reduced from various kinds of iron ores.

For the industrial purpose, it is necessary to prevent the reoxidation of reduced iron such as sponge iron. Then the reoxidation behaviors of those reduced irons produced from various kinds of iron ores are to be studied. Furthemore, the relation between the reoxidation behaviors of reduced irons and the physical and chemical properties of original iron ores is to be studied.

Now, the various kinds of iron ores, such as hematite, magnetite, limonite, iron sand, pyrite cinder, laterite and ferric oxide were used for the present experimets.

The temperature of reduced irons is elevated rapidly during the reoxidation because of the exothermic reaction of oxidation of metallic iron. Therefore, strictly speaking, its system must be analyzed as a heterogeneous system. Moreover, the characteristics of reduced irons may be changed as the reoxidation proceeds. Now, since the changes of temperature of reduced irons is significant for the analysis of the reoxidation process, they are measured by the thermocouple settled at the vessel of the samples. However, considering the pore volume decrease resulted from the formation of oxide films on the pore surfaces of reduced irons, the exact analysis of the reoxidation behaviors is very difficult. Hence, in the present study the experimental results are analysed only quantitatively.

Since the reduced iron is porous, the reactivity of reduced irons is almost controlled by its specific surface area which is measured by the BET method.

The reoxidation degree is defined as follows:

$$\text{Reoxidation degree } (\%) = \frac{A}{B \times \dfrac{2 \cdot M_O}{3 \cdot M_{Fe}}} \times 100$$

A: weight increase by reoxidation (g)
B: total weight of iron (g)

1.2. Materials

The specimens used in the present work are ferric oxide, iron sand, laterite, pyrite cinder, and various iron ores such as Cotabato, Temangan, Goa, Santa Fé and Kennedy Lake.

TABLE 1. Chemical Composition of Ores

Ore	T.Fe	FeO	Fe_2O_3	SiO_2	Al_2O_3	CaO	MgO	S	P	Cu	C.W.
Temangen	53.13	0.14	75.92	3.36	1.06	0.24	0.05	0.022	0.058	—	—
Goa	58.78	1.58	82.42	2.70	4.87	0.06	0.19	0.037	0.062	0.002	6.05
Cotabato	56.55	1.08	79.65	3.64	0.59	0.16	tr.	0.420	0.330	—	12.73
Santa Fe'	69.18	28.47	67.27	0.94	0.78	—	—	—	—	—	0.30
Kennedy Lake	65.17	26.82	63.39	2.10	0.78	0.78	2.26	0.054	0.016	0.003	0.75
Laterite	61.1	0.688	87.3								
Pyrite cinder	54.0	5.0	71.6								
Iron sand	53.6	29.6	43.7								
Fe_2O_3	70.0										

Their chemical composition are shown in Table 1. The powders of the size between 42 and 65 mesh were used in experiments.

1.3. Experimental apparatus and procedures

The measurements of weight change by reduction and reoxidation were made using the digital balance shown in Fig. 1. The system for the gas purification are shown in Fig. 2. The reaction gases were preheated by passing through the packed bed of alumina particles in the lower position of the reaction tube. The platinum vessel of diameter 20 mm for the powders of iron ores were shown in Fig. 3.

At least 90% of the combined water contained in iron ores was eliminated

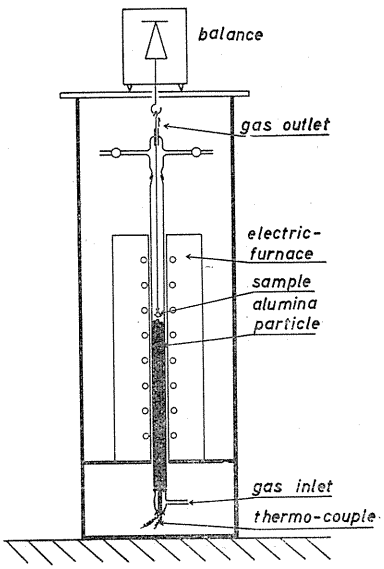

FIG. 1. Experimental Apparatus.

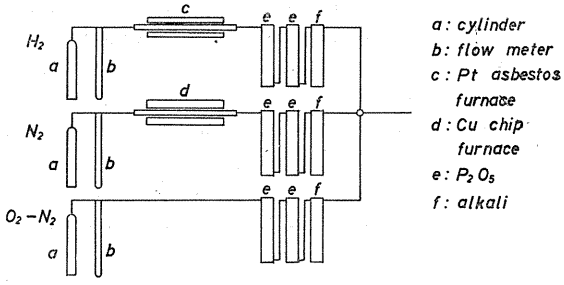

FIG. 2. Flow diagram for gas system.

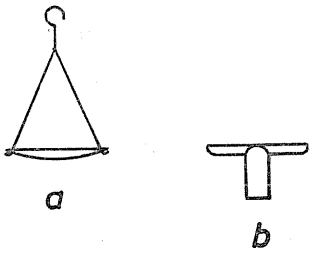

FIG. 3. Vessel.

by heating them for 30 min at 400°C before reduction.

The iron ores were reduced by hydrogen and then cooled or heated at the definite reoxidation temperature under the same atmosphere. Then, the atmosphere was purged with nitrogen and the reduced irons were reoxidized by N_2-O_2 gas mixtures containing various potentials of oxygen.

The temperature of reoxidation was chosen as the lower temperature than that of reduction, 400°C.

Furthermore, the reduced irons should be reoxidized by the sufficiently low oxygen potential under which the temperature rise could be negrigible, compared with the reoxidation temperature. Consequently, the oxygen potentials of the N_2-O_2 gas mixtures were chosen as 5% and 8% oxygen except some special cases.

1.4. Experimental Results

The experimental conditions affecting the reoxidation of reduced iron are as follows; 1) geometries and amounts of packed bed of powders, 2) velocities of reacting gas flowing around samples, 3) oxygen potentials, 4) characteristics of original iron oxides or kinds of iron ores, 5) reduction temperatures, 6) kinds and potentials of reducing gas, 7) histeresis of reduced irons after reduction, and 8) reoxidizing temperatures are concerned.

The experimental conditions, 1), 2) and 3) are related with the transport of oxygen from gas bulk to samples and the release of heat from the sample. The experimental conditions, 4), 5), 6) and 7) are related with the characteristics of reduced irons. The experimental conditions, 3) and 8) are related with the reaction of reoxidation.

In the present study, hydrogen was used for the reducing gas. In order to ascertain the effects of the histeresis of reduced irons, some reduced irons were heated at the higher temperature than their reduction temperature. It seems probable that the experimental condition 7) is significant for the purpose of the prevention of the reoxidation of reduced irons. Therefore, the studies on the effects of the experimental conditions 7) on the reoxidation are expected in the future.

Present work shows the results of experiments and discussions concerning the experimental conditions, 1), 3), 4), 5), 7) and 8).

1.4.1. Effects of geometries and amounts of the packed bed of iron oxides on the reoxidation

Since the powders of iron ores were packed in the vessel shown in Fig. 3 a, the geometry of sample was similar to that of a convexlens. Oxygen consumed by the reoxidation is transported through the upper surface of the packed bed.

The heat evolved by the reoxidation is transfered from the upper surface of the packed bed to the surroundings upward and also is conducted through the vessel downward to the atmosphere.

The amounts of packed bed were controlled by changing the weight of powders of ferric oxide.

Various amounts of iron powders reduced from ferric oxide by hydrogen at 600°C were reoxidized in nitrogen containing 4.9% oxygen at 400°C. Their reoxidation curves were shown in Fig. 4, which showed that the reoxidation degree increased with increasing amounts of ferric oxide. The temperature

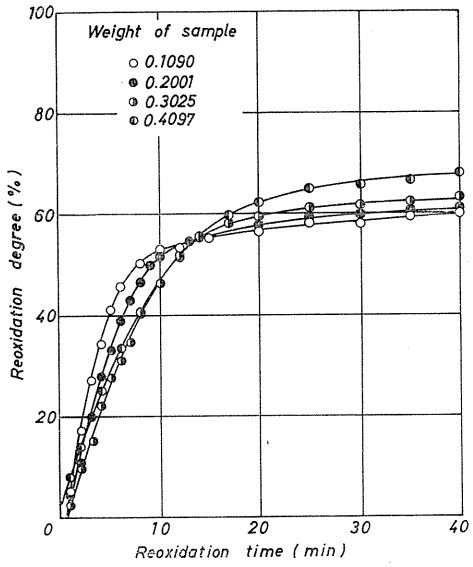

FIG. 4. Effect of weight of sample on the reoxidation degree.

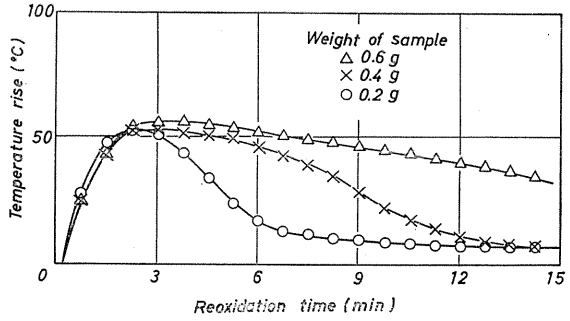

FIG. 5. Temperature rise during reoxidation of sponge-iron powders of various amounts.

changes during the reoxidation of various amounts of reduced irons were shown in Fig. 5. With increasing the amount of the sample, the reduced irons would be heated at higher temperatures due to the reoxidation for increasing time and would be reoxidized to the higher reoxidation degree.

1.4.2. Effect of oxygen potential on the reoxidation

The effect of the oxygen potential on the reoxidation was investigated with the iron powders reduced from ferric oxide. Both of the rate of reoxidation and the reoxidation degree increased with increasing the oxygen potential, as shown in Fig. 6. The increase of the initial rates of reoxidation which are taken from the tangents drawn to the reoxidation curves at the starting time is proportional to the oxygen potential, as listed in Table 2. The changes of temperature during the reoxidation with nitrogen containing various oxygen potentials were shown

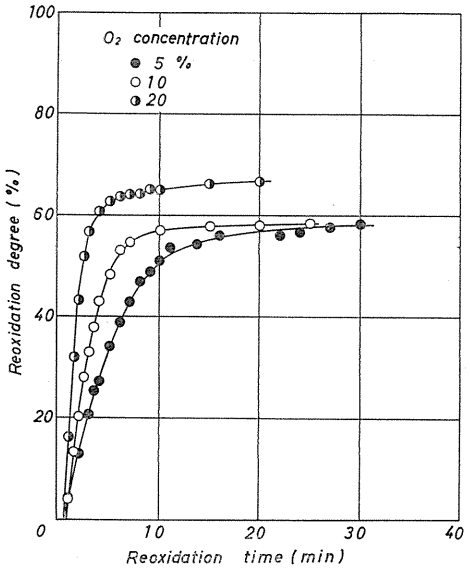

FIG. 6. Effect of oxygen concentration on the reoxidation degree. (Reduction: 500°C, Reoxidation: 400°C)

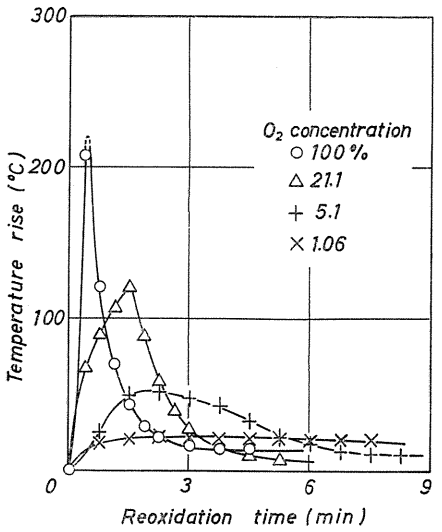

FIG. 7. Temperature rise during the reoxidation of sponge-iron powders. (Reduction: 600°C, Reoxidation: 400°C)

TABLE 2. Effect of Oxygen Pressure on Initial Reoxidation Rate (at 400°C) of Sponge Iron Reduced at 600°C

Oxygen pressure	Initial re-oxidation rate
0.0021 atm	0.52 mg•sec^{-1}
0.0106 〃	1.9 〃
0.0516 〃	7.4 〃

in Fig. 7. The maximum value of the temperature of each curve increases with increasing the oxygen potential.

The oxygen potential in the bulk of the oxidizing gas mixture limits the transfer rate of oxygen by which the rate of reoxidation on the pore surface is affected. The initial rate of reoxidation may increase in proportional to the oxygen potential if the rate limitting step of the reoxidation is the gas transport.

1.4.3. Effect of reduction temperature on the reoxidation

The iron powders reduced from ferric oxide at the temperature between 400° and 800°C were reoxidized with nitrogen containing 8.4% oxygen at 400°C. It is remarkably observed that the iron powders reduced in the neighbourhood of 600°C are reoxidized to the maximum reoxidation degree as shown in Fig. 8. The initial reoxidation degree increased till 600°C and decreased over 600°C with increasing the reduction temperature.

Furthermore, the effect of the reduction temperature on the reoxidation were investigated with the iron powders reduced from various iron ores. These results were summarized in Fig. 9 where the reoxidation degree was represented by the reoxidation degree at the reoxidation time of 30 min. Those results show that the most reduced iron powders reduced in the neighbourhood from 600° to 700°C are reoxidized to the maximum reoxidation degree except a few iron ores.

The reoxidation degrees of those iron powders reduced from some particular iron ores, such as laterite and iron sands, increase with increasing the reduction temperature even over 800°C. The iron powders reduced from Temangan ore at 400°C were reoxidized to the higher degree than that of iron powders reduced at 700°C.

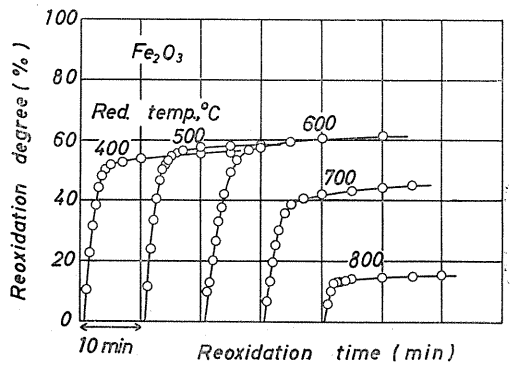

FIG. 8. Reoxidation curves of sponge-iron powders reduced at various temperatures.

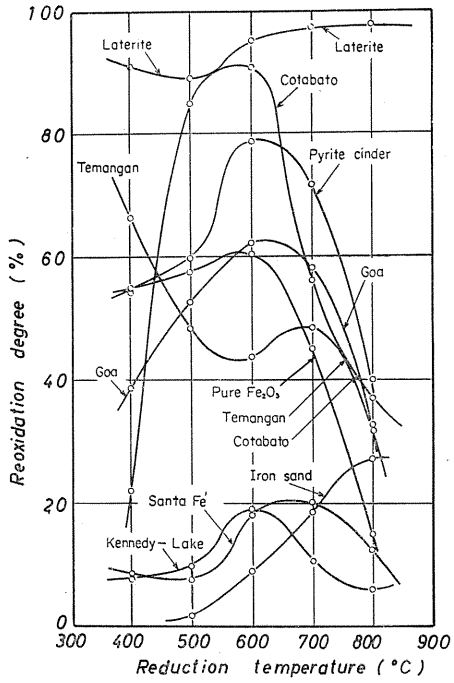

FIG. 9. Effect of reduction temperature on the reoxidation degree of various iron ores. (Reoxidation: 400°C, 8.4%O_2)

1.4.4. Effect of reoxidation temperature on the reoxidation

The effect of the reoxidation temperature on the reoxidation degree was examined for those iron powders which were reduced from ferric exide at 400°C or 600°C. They were reheated in the same reducing atmoshere at the corresponding temperature for 10 min and then reoxidized with nitrogen containing 8.4% oxygen. The relationships between the initial reoxidation degrees of iron powders and the reoxidation temperature were shown in Fig. 10.

So far as the results shown in Fig. 10 are concerned, the reduced iron powders are reoxidized to the maximum reoxidation degrees when they are reoxidized at the

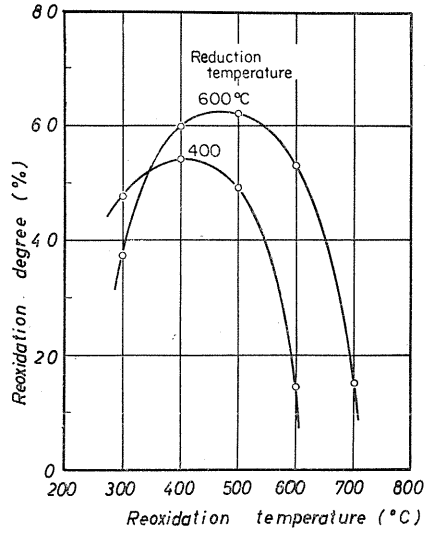

FIG. 10. Effect of reoxidation temperature on the reoxidation degree of sponge-iron powders reduced at 400° or 600°C.

temperatures which are slightly lower than the reduction temperature.

In addition, the maximum reoxidation degree of iron powders reduced at 600°C is larger than that of iron powders reduced at 400°C.

1.4.5. Effect of histeresis of reduced iron powders after reduction on the reoxidation

The iron powders reduced from ferric oxide at 600°C were reheated to 700°C in the same reducing atmosphere and kept for various periods up to 3 hr. Then, those iron powders were reoxidized with nitrogen containing 4.9% oxygen at 400°C. The reoxidation curves were shown in Fig. 11.

It is to be noticed that the iron powers reduced at 700°C should be reoxidized to the higher reoxidation degree than those iron powders reheated at 700°C after reduced at 600°C.

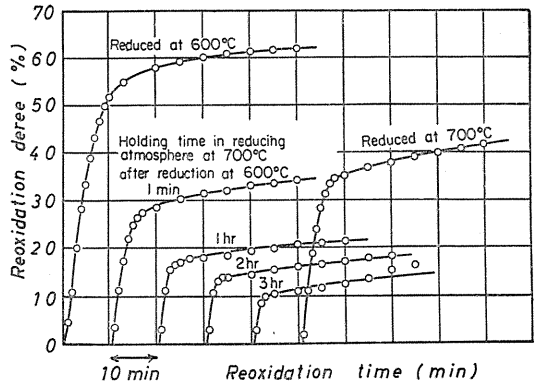

FIG. 11. Effect of heating after reduction on the reoxidation degree.

1.5. Discussions

1.5.1. Relation between characteristics of reduced iron powders and reoxidation degrees

The reoxidation behaviors of iron powders reduced are affected by the experimental conditions such as those described in 1.4. On the other hand, the reactivity of reduced iron powders is represented by the characteristics such as 1) specific surface areas, 2) distortions of lattice and 3) pore size distributions.

Here, those characteristics, 1), 2) and 3), should be determined by 4), 5), 6) and 7) of the experimental conditions described before.

The specific surface areas of iron powders reduced from ferric oxide at the temperature between 400° and 800°C were measured. They decrease with increasing the reduction temperature, as shown in Fig. 12. Here, krypton was used as the adsorption gas to measure the specific surface area of iron powders reduced at 700° or 800°C because of their smaller surface areas. For those iron powders reduced at the temperature lower than 600°C, nitrogen was used as usual.

Although the specific surface areas of iron powders reduced from iron ores were not measured, they would decrease with increasing the reduction temperature as those from ferric oxide.

According to the previous works[1)2)], the mean size of the pores of reduced irons increases with increasing the reduction temperature. Then, it is necessary to know how are the effects of those characteristics of reduced iron powders on their reoxidation degrees.

Generally, the reoxidation degree should increase with increasing the specific surface area, assuming that the same thickness of oxide films is formed uniformly on the pore surface.

The distrotion of the lattice increases the heat content of reduced irons and consequently promotes the reoxidation. The distortion decreases with increasing the reduction temperature as the specific surface area[3)].

The volume of metallic iron becomes larger as a metallic iron is oxidized to the higher degree. If the volume of a metallic iron is to be 1, the volume of each iron oxide is shown as follows;[4)]

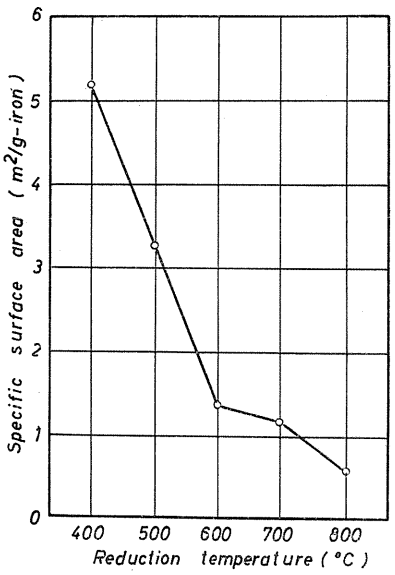

FIG. 12. Specific surface area of sponge-iron powders reduced at various temperatures.

$FeO_{1.055\sim1.19}$: 1.68～1.76
Fe_3O_4 : 2.10
Fe_2O_3 : 2.14

If the dimensions of a reduced iron is constant, the pore sizes of the reduced irons become smaller as it is reoxidized to the higher degree. Smaller pores

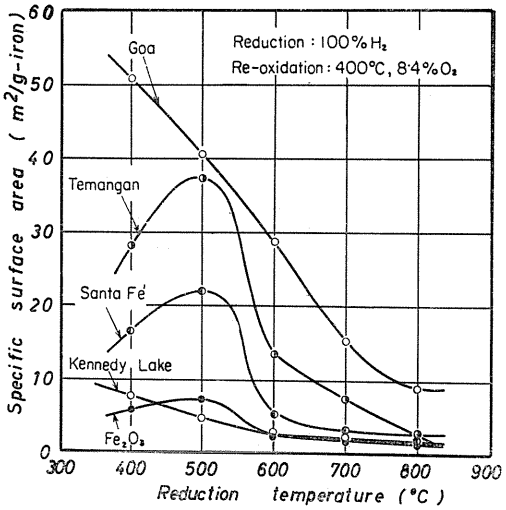

FIG. 13. Specific surface area of reoxidized sponge-iron powders reduced at various temperatures.

may be filled with iron oxides formed during the reoxidation. The surfaces of pores filled with iron oxides can not contribute to the further reoxidation. Therefore, the increase of the existence of rather larger pores except such smaller pores contributes to the increase of reoxidation degree.

Although the effects of the pore size distribution could not be shown strictly by the experimental results, the specific surface areas of reduced iron powders after the initial rapid reoxidation were measured for the iron powders reduced at various temperature. The results are shown in Fig. 13. Some of these curves show the maximum value in the neighbourhood of 500°C, although the specific surface areas of reduced iron powders decrease with increasing the reduction temperature. This results may suggest that the oxide layer formed on the pore surface narrowers its pore or fills some pores to decrease the specific surface area.

1.5.2. Relations between reoxidation degrees and experimental conditions

1.5.2.1. Relation between reoxidation degrees and reduction temperatures

The specific surface areas and the distrotion of lattice of reduced irons are the characteristics which decrease the reoxidation degree with increasing the reduction temperature.

On the other hand, the pore size distribution of reduced irons is a characteristic which increases the reoxidation degree with increasing the reduction temperature.

Considering those reasons, the reoxidation degree would become maximum for the iron powders reduced at 600°~700°C by those characteristics.

1.5.2.2. Relation between reoxidation degree, and reoxidation temperature and oxygen potential

Besides the above characteristics of the reduced iron, the reoxidation temperature and the oxygen potential should be important factors which control the reaction of reoxidation.

The mechanism of the reoxidation of the reduced iron powders must be analysed in order to understand the effect of these experimental conditions on the reoxidation degree.

As described in chapter 2, the logarithmic rate law is valid to the reoxidation of reduced iron powders. The dependence of the rate constant of the logarithmic law on the reoxidation temperature is represented by the Arrhenius relation. The rate constant hardly increases with the oxygen potential. But, since the temperature of reduced iron powders rises with increasing the oxygen potential due to the heat of reoxidation, the increase of oxygen potential behaves as the increase of the reoxidation temperature.

When the reoxidation temperature is raised, not only the effect of the accerelation of reoxidation but also the effect of the sintering of reduced iron powders before the reoxidation must be considered. If the effect of the sintering on the reoxidation is stronger than the effect of the accerelation of reoxidation, the reoxidation degree may decrease with increasing the reoxidation temperature.

The increase of oxygen potential raises the temperature of reduced iron powders during the reoxidation. However, it is to be noticed that the reoxidation and the sintering are proceeding simultaneously even during the rise of temperature due to the heat of reoxidation. This is different from the effect of

the increase of the reoxidation temperature where the reduced iron powders are sintered before they are reoxidized.

As described already, the temperature of reduced iron powders increases during the reoxidation with increasing the oxygen potential. Therefore, the increase of the oxygen potential accerelates the reoxidation, although the increase of temperature acts as the sintering of the reduced iron powders.

1.5.2.3. Relation between reoxidation degrees and reducibilities of various iron ores

Summarizing the present results, it is found that the magnetite ores are very difficult to reduce and the iron powders reduced from them are reoxidized only to the lower reoxidation degree such as 20%.

Hematite and limonite ores are reduced and the iron powders reduced from them are reoxidized even up to the higher reoxidation degree such as 95%.

Although laterite is more difficult to reduce in the lower temperature, compared with hematite, the iron powders reduced from laterite are reoxidized exceptionally to the higher reoxidation degree than that of hematite.

1.6. Conclusions

The reoxidation behaviors of iron powders reduced from ferric oxide and various iron ores at the temperature range from 400° to 800°C were studied. Generally speaking, it may be necessary to study the heat transfer during the reoxidation, since the reoxidation of reduced iron powders is very exothermic and their temperature changes during the reoxidation. Here, the elevation of temperature changes the characteristics of reduced iron powders, and also the products of reoxidation, that is, iron oxides change the characteristics of porous iron powders. However, the quantitative analysis of the reoxidation behaviors of reduced iron powders is very difficult. Therefore, in the present study the reoxidation behaviors are mainly analysed qualitatively.

Following conclusions are obtained.

(1) The iron powders reduced from ferric oxide and various iron ores at 600°~700°C are reoxidized to the maximum reoxidation degree among the iron powders reduced at 400°~800°C.

(2) The reoxidation degree increases with increasing the oxygen potential and increasing the amounts of powders.

(3) The reduced iron powders reheated at the higher temperatures than the reduction temperature are reoxidized only to the lower reoxidation degree than the iron powders reduced at the same reheating temperature.

(4) The reoxidation degrees of iron powders reduced from ferric oxide and various iron ores are as follows.

The iron powders reduced from limonite have very large specific surface areas and they are reoxidized to the high reoxidation degree such as 90%. The iron powders reduced from hematites are reoxidized to the considerably high reoxidation degree such as 40~60%. The iron powders reduced from magnetites have small specific surface areas and they are reoxidized only to the lower reoxidation degrees such as 10~20%.

(5) The specific surface areas, the distortion of lattices, and the pore size distributions could be considered as the characteristics of reduced iron powders

which determine their reoxidation degrees. In addition, the reoxidation temperature and the oxygen potential are considered to be the experimental conditions which affect the reoxidation degree. The reoxidation behaviors could be analysed qualitatively with those characteristics of reduced iron powders and these experimental conditions.

(6) As a factor concerning the reoxidation of iron powders, the temperature change during the reoxidation is especially important when the reduced iron poweders are reoxidized at the lower temperatures such as the room temperature.

Chapter II. Kinetics of Reoxidation of the Sponge-Iron Powders

2.1. Introduction

In the previous Chapter, the effects of the various factors on the reoxidation degree were explained. Here, the kinetic study of the reoxidation behaviors of reduced iron powders is desired.

There are few works on the rate of reoxidation of metallic iron powders in the field of catalyzer[5)6)], however, the metallurgical kinetic study has not yet been reported.

Now, considering those physical properties of the reduced iron powders obtained from some microscopic observations, X-ray diffraction analysis and the specific surface areas, the process of reoxidation is analyzed.

2.2. Materials

Brazilian hematite iron ore and ferric oxide were used in the present experiment. Their chemical compositions are shown in Table 3.

TABLE 3. Chemical Composition of Iron Ores

	P.Fe	SiO_2	Al_2O_3	S	P	Cu	Mn
Brazil	66.10	2.25	1.47	0.018	0.041	0.002	0.08
Fe_2O_3	70.0	—	—	—	—	—	—

	CaO	MgO	TiO_2	FeO	Fe_2O_3	As	C.W.
Brazil	0.16	0.18	0.12	1.04	93.36	0.002	1.06

2.3. Experimental apparatus and procedures

The auto-recording type thermobalance shown in Fig. 14 was used for the present experiment. The platinum vessel for the specimens is 20 mm diameter and 2 mm depth. The temperature change of the specimen can be determined by a thermocouple settled beneath the vessel through the supporting rod of the balance.

The experiment was carried out with the reduction experiment and the reoxidation experiment continuously.

The experimental procedure is as follows: 0.2 g ferric oxide or 0.3 g Brazilian hematite was settled in the vessel, then the reaction chamber together with the inside of the balance was filled with nitrogen. The reduction was carried out in the

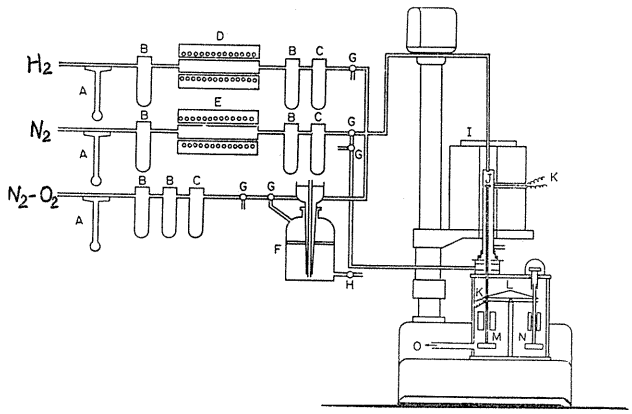

A: Flow meter B: P_2O_5 C: Soda-asbestos
D: Pt-asbestos E: Cu-chip F: Gas reservoir
G: 3-way cock H: 2-way cock I: Electric furnace
J: Vessel K: Thermo-couple L: Balance
M: Magnet and solenoid coil
N: Differential core and differential transformer
O: Vacuum pump

FIG. 14. Experimental apparatus.

hydrogen atmosphere at a definite temperature and then the temperature was adjusted to the reoxidation temperature. The reaction chamber was then evacuated and then nitrogen-oxygen gas mixture was introduced for the reoxidation of the sample. If the sampling during the reoxidation was necessary, the atmosphere in the chamber was evacuated and the sample was quenched to the room temperature.

2.4. Experimental results and discussions

2.4.1. Processes of reoxidations

A large number of studies have been made on the oxidation of metals both experimentally and theoretically. Almost all of these were carried out on the lumps or plates of metals. On the very porous and active powdery metals as in this work, a few studies have been made from the catalystic point of view.

In principle, the theories and the rate laws established on the oxidation of metals would be also applicable to the reoxidation of reduced irons such as sponge irons. However, the change of reaction interface, the filling of pores of reduced irons by iron oxides formed, the variation of lattice defects and etc. take place during the reoxidation of reduced irons. Hence, the reoxidation behaviors of reduced irons are very complex and various observations concerning reoxidation are necessary for the correct analysis of reoxidation behaviors. Then, microscopic observations of the reduced irons reoxidized partially, the measurement of specific surface area by the BET method and the identification and the estimation of relative integrated intensities of iron oxides formed in reoxidation by X-ray analysis were investigated on the reoxidation of the reduced irons.

2.4.1.1. Microscopic observation of the reduced irons during the reoxidation

Microscopic observations were carried out on the reduced irons (reduced from Brazilian ore with hydrongen at 400°C) reoxidized by nitrogen containing 4.7% oxygen for various periods at 400°C as shown in Photo 1.

The thickness of iron oxide layers formed on the pore surface of reduced irons increases as its reoxidation proceeds. It is noteworthy that some internal pores are filled with iron oxides formed by the reoxidation, as shown in Photo 1-c, d, e. Since the greater part of iron oxide layers observed in polished section is grey, almost all of iron oxide layers are appeared to be magnetite. Those very thin white layers observed in the surface part of the iron oxide layers as shown in Photo 1-e are regarded as hematite. The relation between the photographs shown in Photo 1 and the reoxidation degree was shown in Fig. 15.

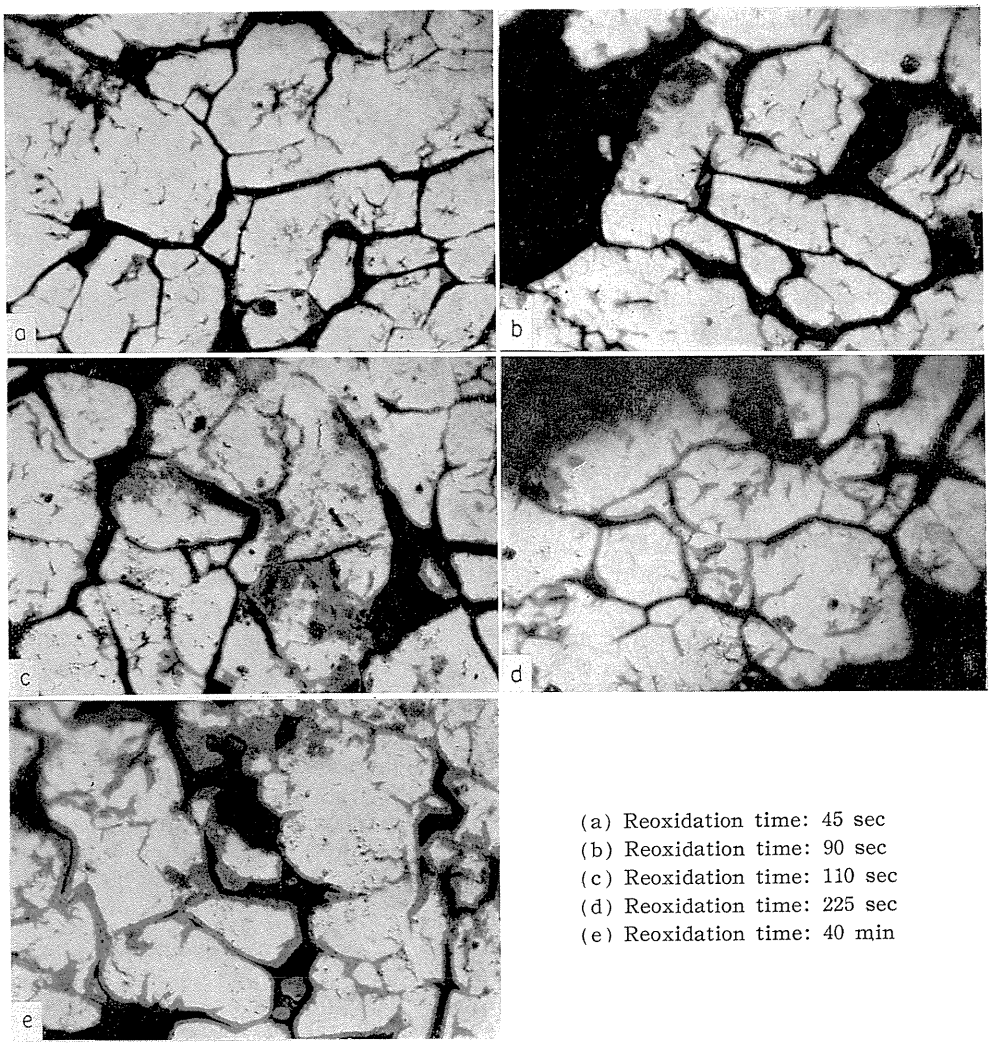

(a) Reoxidation time: 45 sec
(b) Reoxidation time: 90 sec
(c) Reoxidation time: 110 sec
(d) Reoxidation time: 225 sec
(e) Reoxidation time: 40 min

PHOTO 1. Microscopic observation of reoxidation process of sponge-iron. (×600)

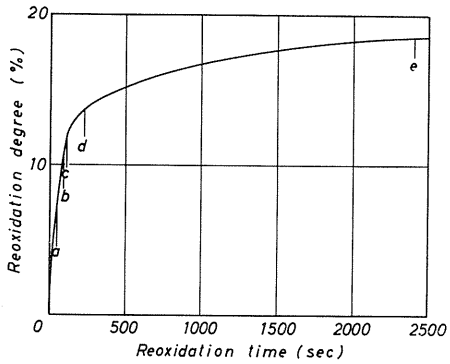

FIG. 15. Relation between the reoxidation time and the reoxidation degree of iron powders reduced from Brazilian ore. a, b, c, d, and e correspond Photo 1-a, 1-b, 1-c, 1-d, and 1-e.

2.4.1.2. The changes of the specific surface area and relative integrated intensities of iron oxides formed during reoxidation

In order to clarify the reoxidation behaviors of very porous and active reduced irons, it is necessary that the changes of the specific surface area and the amount of each iron oxide during the reoxidation are determined experimentally. For this purpose, those iron powders reduced from ferric oxide by hydrogen at 600° (Figs. 16 and 17) and 800°C (Fig. 18) were reoxidized at 400°C by N_2-O_2 mixtures containing 4.7% (Fig. 16) and 1.06% (Figs. 17 and 18) oxygen. The results are shown in Figs. 16, 17 and 18. Here, the reoxidation process are considered by dividing into the initial stage and the later stage as described later.

The shift from the initial stage to the later stage is to be considered in the relations with the changes of the specific surface area, the amounts of various iron oxides and the reoxidation degree.

The results shown in Fig. 16 are considered in relation to the change from the initial stage to the later one. The specific surface area shows the maximum value in the initial stage, and shows nearly constant value in the later stage. The amount of magnetite as a component of oxides layer formed in reoxidation increases rapidly in the early part of the initial stage, while the amount of hematite increases gradually. However, wustite was not detected by the X-ray analysis.

The increase of the specific surface areas during reoxidation of reduced iron powders would be attributed to the defects formed as clacks and blisters. On the contrary, the decrease of the specific surface area would be resulted from the filling of small pores with iron oxides formed during reoxidation. The effect of these two factors yields the maximum value in the change of the specific surface area.

Although Fig. 17 shows the similar results as shown in Fig. 16, the results shown in Fig. 18 are somewhat different. Namely, the specific surface area increases even in the later stage and only magnetite is detected by X-ray analysis. Hematite is never obserbed.

Those results shown in Figs. 16, 17 and 18 are considered as follows.

The specific surface area takes the maximum value in the initial stage of the reoxidation as shown in Figs. 16 and 17, but increases even in the later stage in Fig. 18. This fact suggests that the rapid decrease of the rate of reoxidation are independent of the changes of the specific surface area, but they

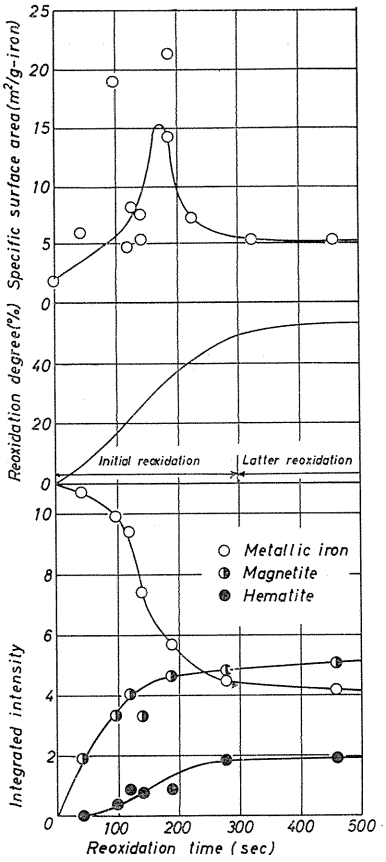

FIG. 16. Changes of specific surface area, reoxidation degree and integrated intensity of iron oxides by reoxidation time.

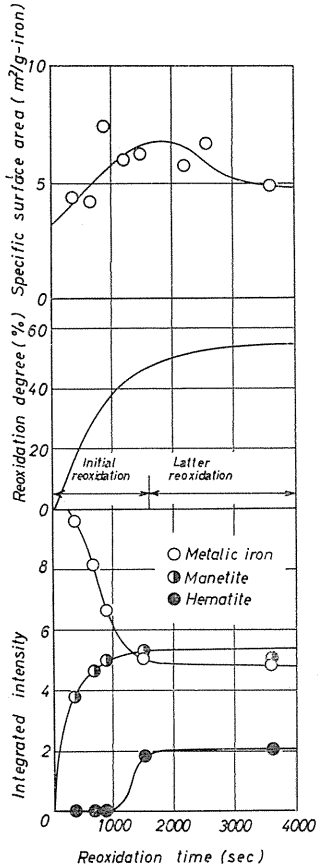

FIG. 17. Changes of specific surface area, reoxidation degree and integrated intensity of ion oxides by reoxidation time.

are controlled by the reoxidation degree.

The relation between the change of the rate of reoxidation and the change of the amount of various iron oxides are considered. As described already, the amount of magnetite increases rapidly in the initial part of the initial stage and that of hematite increases in the later part of the initial stage. Therefore, the increase of hematite appears to decrease the rate of reoxidation, however, it is not reasonable that the formation of hematite should result in the decrease of the rate of reoxidation.

Now, let us refer to the oxidation of metallic iron plate.

At first, the change of volume of each iron oxide must be considered when the metallic iron is oxidized. The ratios of the volume of each iron oxide to that of original metallic iron are as follows; $FeO_{1.055\sim1.19}$: 1.68 1.76, Fe_3O_4: 2.10 and Fe_2O_3: 2.14[4]

Since the volume of iron oxide becomes larger as the oxidation degree

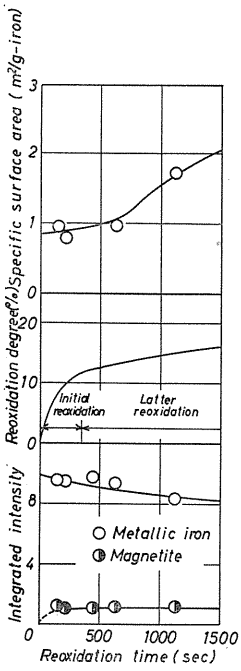

FIG. 18. Changes of specific surface area, reoxidation degree and integrated intensity of iron oxides by reoxidation time.

increases, some stresses may be created at the interface between metallic iron and iron oxides layer or within the iron oxide itself. Hence, the clacks or blisters are broken out in the iron oxide layer and the surface area would increase as the oxidation proceeds.

In the present case, the surface area would never decrease in the process of oxidation.

It has been reported[7)~15)] that when metallic iron is oxidized below 570°C, the main component of iron oxides layer formed is Fe_3O_4 and some amount of hematite is obserbed, too. Above 600°C, however, the main component is wustite, and some amount of magnetite and hematite are also formed. In this investigation where the reduced iron is oxidized at 400°C, it is observed that the main component is magnetite and smaller amount of hematite is also formed. This is in good agreement with the above reports.

However, Davies and co-workers[16)] has reported some different results on the oxidation of metallic iron at the temperature between 225° and 325°C.

Their results shows that only Fe_2O_3 is formed at 225°C and smaller amount of Fe_3O_4 is also formed in further oxidation. At 300°C, both Fe_3O_4 and Fe_2O_3 were formed in about equal amount.

As concerns the ratio of the amount of each iron oxide formed, it has been reported that the ratio of thickness of each iron oxide is independent of oxidation time. At 700°C, the ratios of the thicknesses of FeO-, Fe_3O_4- and Fe_2O_3-layers have been reported[12)17)] to be 100 : 10 : 1 or 100 : 5 : 1, and also to be independent of oxidation temperature.

However, those values at the lower temperatures such as 400°C have never been investigated.

When the metallic iron plate is oxidized, such rapid change of the reoxidation rate as observed on the reduced iron is not observed. Also, the slight deviation from the parabolic rate law is obserbed[18)] in the early stage of oxidation probably due to the heat of oxidation. On the other hand, the remarkable change of the reoxidation rate observed on the reduced iron may be resulted from the remarkable temperature increase at the biginning of the reoxidation.

According to Wagner's theory[19)], iron atom is dissociated into iron ion Fe^{2+} and electrons and then iron ion Fe^{2+} diffuses towards the surface of the iron oxide layer. On the other hand, oxygen atom takes the electrons and diffuses inwards as an oxygen ion O^{2-}.

As well known[7)10)20)21)], wustite is a p-type semi-conductor and contains many vacancies in partial lattice of iron ions through which iron ion diffuses. Magnetite is somewhat similar to wustite and iron ion diffuses also through the vacant sites of iron ions. Hematite is a n-type semi-conductor and oxygen ion diffuses through the vacant sites of oxygen partial lattice.

Since iron ion Fe^{2+} is smaller than oxygen ion; Fe^{2+}: 0.75 Å, Fe^{3+}: 0.60 Å and O^{2-}: 1.40 Å[22)], iron ion Fe^{2+} can diffuse more rapidly than oxygen ion. If the diffusion process is rate limitting step, the reoxidation rate in $Fe \rightarrow FeO \rightarrow Fe_3O_4$ is controlled by the diffusion of iron ion Fe^{2+} and the reoxidation rate in $Fe_3O_4 \rightarrow Fe_2O_3$ is controlled by the diffusion of oxygen ion.

Therefore, $Fe \rightarrow FeO \rightarrow Fe_3O_4$ oxidation should be more rapid than $Fe_3O_4 \rightarrow Fe_2O_3$ oxidation. Another paper shows that the initial rapid reoxidation of reduced iron is $Fe \rightarrow FeO \rightarrow Fe_3O_4$ oxidation and the later slow reoxidation is $Fe_3O_4 \rightarrow Fe_2O_3$ oxidation.

Furthermore, if the diffusion process of ions were rate limitting step, the reoxidation rate would be directly proportional to the specific surface area. Nevertheless, the initial reoxidation rate of iron powders reduced at various temperatures are independent of the specific surface areas of the reduced iron. Therefore, the rapid decrease of reoxidation rate can not be attributed to the change from diffusion of Fe^{2+} to diffusion of O^{2-}.

2.4.2. Rate of reoxidation

The rate of reoxidation of reduced irons is very rapid in the initial stage but decreased rapidly in the later stages. In order to study the rate of overall reoxidation, the mechanism of the later stages of reoxidation must be analysed where the oxidation process of metallic iron on the pore surface should be considered to be rate limitting step. Successively, the rate analysis of the initial rapid oxidation is desired.

2.4.2.1. Rate of reoxidation in the later stages

The rate laws applied generally in the oxidation of metals are summarized

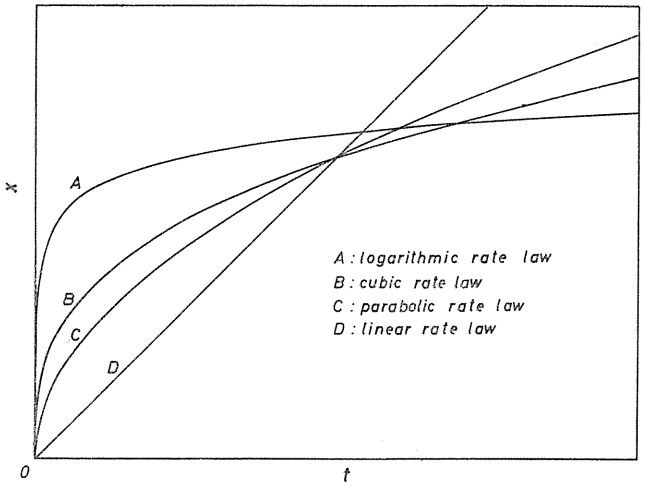

FIG. 19. Representation of various rate laws.

TABLE 4. Representative Rate Law

Rate law	Relation between x and t
Linear rate law	$x=k'\cdot t$
Parabolic rate law	$x^2=k'\cdot t$
Cubic rate law	$x^3=k'\cdot t$
Logarithmic rate law	$x=k'\cdot\log(t+t_0)$

in Fig. 19 and Table 4[23]. Any of these rate laws could be applied to the reoxidation of reduced irons. The logarithmic rate law is substantiated to be applied to the later stages of reoxidation.

The reoxidation curves are shown in Fig. 20 representing the reoxidation time in common logarithms, when the iron powders reduced from ferric oxide with hydrogen at 800°C were reoxidized in the nitrogen containing 4.7% oxygen at the temperature 300° to 800°C.

The logarithmic rate law can be applied to the present results except the initial period up to 300~500 sec. The value of x shown in Table 4 is not weight increase but thickness of oxides layer. In the present work, the main component of iron oxides layer is Fe_3O_4 and a small amount of Fe_2O_3 is observed. It is further observed that 89% of total oxidation proceeds during the reaction, $Fe\rightarrow Fe_3O_4$ and residual 11% during $Fe_3O_4\rightarrow Fe_2O_2$, respectively. Considering these facts, the thickness of iron oxides layer on the pore surface of reduced irons is in the almost linear relation with weight increase in reoxidation.

Now, the logarithmic rate law is written in Eqs. (1) and (2)

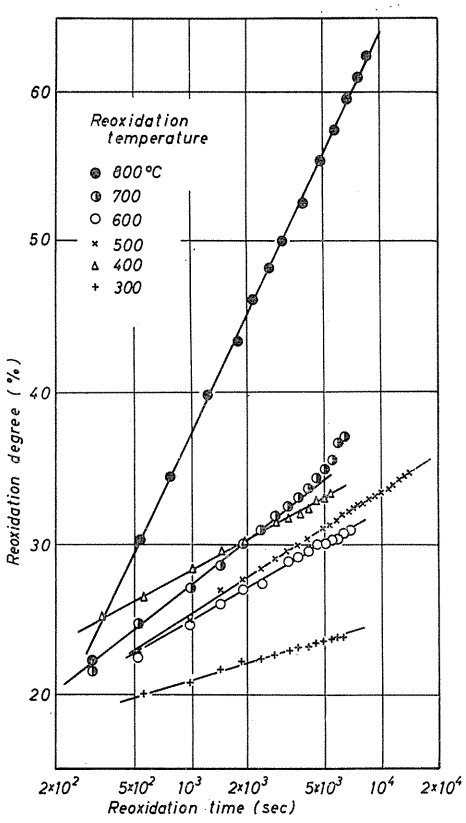

FIG. 20. Logarithmic plot of reoxidation curves at various temperatures.

$$\Delta m/A = k\log t + \Delta m_0/A \quad (t \geqslant t_0) \tag{1}$$

$$F = \frac{\Delta m}{W\cdot C_{Fe}\cdot(3M_O/2M_{Fe})} = S_w\cdot(2M_{Fe}/3M_O)\cdot k\log t + F_0 \tag{2}$$

The specific surface area of iron powders reduced by hydrogen at 800°C was 0.430 $m^2/g\cdot$iron and the areas of those iron powders reoxidized under the conditions written in Fig. 20 were considerably scattered in the range between 0.43 and 1.1 $m^2/g\cdot$iron. However, the rate constant of the logarithmic rate law ex-

pressed in the Eq. (2), $K' = S_w \cdot \frac{2 M_{Fe}}{3 M_O} \cdot k$ were estimated from the gradients of straight lines shown in Fig. 20. The temperature dependence of K' was also shown in Fig. 21. The values of K' estimated here scatters considerably but it

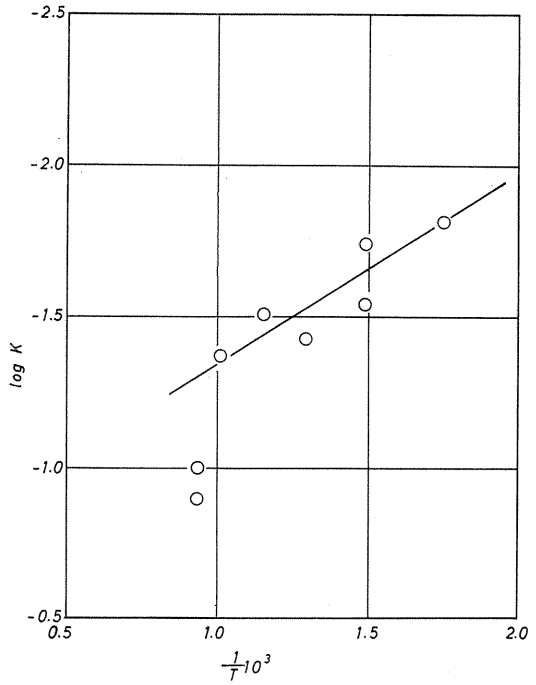

FIG. 21. Arrhenius plots for the reoxidation of iron powders reduced at 800°C, corresponding to Fig. 20.

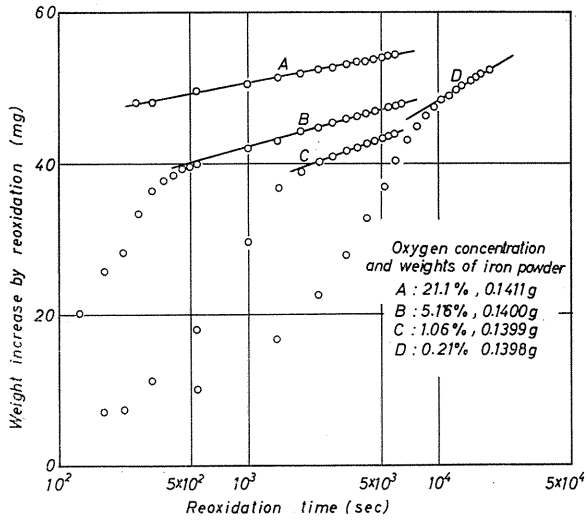

FIG. 22. Logarithmic plots of the reoxidation curves oxidized at various oxygen concentrations.

is unavoidable since the reduced iron is the very active and porous.

The apparent activation energy is estimated to be about 3 kcal/mol which is much smaller than 21.7 kcal/mol estimated from the initial rate of oxidation of iron plate by Measor *et al.*[24]

Successively, in order to investigate the effect of the oxygen potential on the rate constant K', the iron powders reduced by hydrogen at 600°C were reoxidized with N_2-O_2 gas mixtures containing 0.21 to 21.1% oxygen at 400°C. The reoxidation curves were drawn in semi-logarithmic diagram as shown in Fig. 22 which shows the linear relations. It is clearly recognized that the values of K' obtained from the gradients of those straight lines decrease with increasing oxygen potential. This would be resulted from that the effective surface area for reoxidation decreases by the sintering with increasing oxygen potential. Consequently the precise dependence of the oxygen potential was not determined.

Many works[10)13)14)16)25)~29)] which have been published on the oxidation of metallic iron, show that the logarithmic rate law[14)34)35)] is applicable to the oxidation of metallic iron at the lower temperatures below 200°C and the parabolic rate law[10)13)17)18)26)30)~33)] is valid to the oxidation at the higher temperatures above 250°C. However, Davies *et al.*[16] observed in their experiments on the oxidation of metallic iron that logarithmic rate law is obeyed at 175°, 225°, 250°, 375° and 300°C and parabolic rate law at 325° and 350°C. Furthermore, Measor *et al.*[24] studied the initial oxidation of pure iron at the temperature range between 700° and 900°C. They concluded that logarithmic rate law covers the oxidation within the thickness of oxide layer less than about 150000 Å and the rate of oxidation is limitted by the transfer of electron at the oxide-metal interface.

In the present investigation, the mean thickness of iron powders reduced at various temperatures is less than 150000 Å obtained by Measor *et al.*[24] as shown in Table 5.

TABLE 5. Mean Thickness of the Sponge-iron Reduced at Various Temperatures

Reduction temperature	Mean thickness
400°C	250 Å
500	390
600	950
700	1200
800	2300

Generally, it is well known that the logarithmic rate law may be applied to the oxidation of extremely thin films[36)37)]. Mott *et al.* interpretted theoretically the logarithmic rate law as follows; When the oxide formed is the ionic conductor and also the insulator to electron, the transfer of electrons is rate limitting step. Electrons can penetrate the potential barrier without passing over if the oxide layer is very thin. According to the quantum mechanics, the probabilities of the penetration of electrons through the oxide layer is represented by $\exp(-x/x_0)$, where x_0 is the characteristic length. Then, the growing rate of oxide layer is represented by Eq. (3).

$$dx/dt \propto \exp(-x/x_0) \tag{3}$$

Integrating Eq. (3), Eq. (4) is obtained

$$x = x_0 \log(t + t_0) - x_0 \log t_0 \tag{4}$$

Eq. (4) is of logarithmic type.

Against the Mott's theory[36)37)], Measor *et al.*[24)], appling the Uhlig's model[38)39)], showed that the logarithmic rate law should be valid even up to 150000 Å. His conclusion is well agreed with the work by Tylecote[40)] who found that the law was valid up to 10^5 Å in the oxidation of copper.

2.4.2.2. Rate of initial reoxidation

It has been made clear in 2.4.2.1 that the logarithmic rate law is applicable to the later stage of reoxidation. Furthermore, this law is generally accepted to be applied to the initial oxidation of iron plate. Hence, it is reasonable to consider that the rate of the initial stage of reoxidation of the reduced iron should be controlled by the transfer of oxygen from the bulk phase to the reaction interface. Every initial rate of the reoxidation of iron powders reduced at various temperatures is nearly equal, independent of the values of specific surface area as shown in Fig. 23. This result suggests the diffusion control of oxygen molecule.

In the present work, since the reduced iron powders are packed in a columnar vessel shown in Fig. 3 b, the reoxidation proceeds downwards in the axial direction maintaining the reaction interface perpendicular to the axis, as shown in Fig. 24.

Now, the rate of diffusion of oxygen through the gas boundary layer is represented by Eq. (5).

$$J_3 = k_f \cdot (C^b_{O_2} - C^\circ_{O_2}) \tag{5}$$

Then, the rate of diffusion in the reoxidized zone of iron powders packed is shown by Eq. (6), where the transfer by bulk flow is neglected because of the low

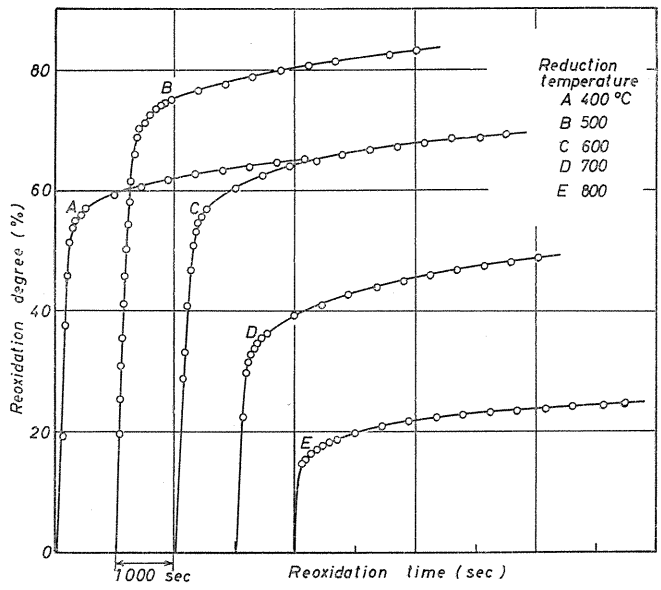

FIG. 23. Reoxidation curves of iron powders reduced at various temperatures. (Reoxidation: 400°C, 5.16% O_2)

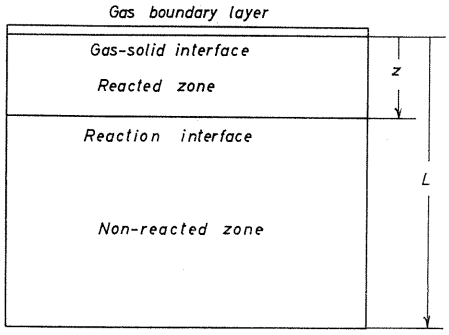

FIG. 24. Schematic profile of reoxidation.

oxygen concentration.

$$J_4 = -D_e \cdot \frac{dC_{O_2}}{dZ} \tag{6}$$

Using $$dC_{O_2}/dZ = -(C^Z_{O_2} - C^0_{O_2})/Z$$

then, Eq. (7) is obtained.

$$J_4 = D_e \cdot \frac{C^0_{O_2} - C^Z_{O_2}}{Z} \tag{7}$$

Those iron powders above the reaction interface are being reoxidized very slowly on the logarithmic rate law after the initial reoxidation and the rate of oxygen consumed in the reacted zone above the interface is represented by Eq. (8).

$$J_5 = \frac{\rho \cdot C_{Fe} \cdot S_w \cdot k}{M_O} d\left(\int_0^Z \log \{t(Z) + t_0\} dZ\right)/dt \tag{8}$$

From the balance of the amount of oxygen, it follows.

$$J_3 = J_4 + J_5 \tag{9}$$

Here, J_5 is very small compared with J_4 until the reaction interface reaches the bottom of vessel, $Z=L$, then

$$J = J_3 = J_4 \tag{10}$$

Here, assuming $C^Z_{O_2} \approx 0$ and substituting Eq. (11) in Eq. (10), it follows,

$$J = \frac{\rho \cdot C_{Fe} \cdot \alpha}{M_{Fe}} \cdot \frac{dZ}{dt} \tag{11}$$

$$\left(R + \frac{D_e}{k_f \cdot L}\right)^2 = \frac{2 \cdot M_{Fe} \cdot D_e \cdot C^b_{O_2}}{\rho \cdot C_{Fe} \cdot \alpha \cdot L^2} \cdot t + \left(\frac{D_e}{k_f \cdot L}\right)^2 \tag{12}$$

where R is the ratio of the reoxidation degree at time t to the initial reoxidation degree, that is, Z/L. Now, the initial reoxidation degree is defined as the reoxidation degree where the logarithmic rate law begins to apply.

Except the starting period of reoxidation, such approximation

$$R \gg D_e/(k_f \cdot L)$$

is written, then it follows,

$$R^2 = \frac{2 \cdot M_{Fe} \cdot D_e \cdot C^b_{O_2}}{\rho \cdot C_{Fe} \cdot \alpha \cdot L^2} t + \text{const} \tag{13}$$

Now, from those results, when the iron powers reduced from ferric oxide by hydrogen at the temperature range between 400° and 800°C were reoxidized at 400°C with nitrogen containing 0.21 to 21.1% oxygen, some typical examples of R^2 vs t plots of these results are shown in Fig. 25. It is found that the linear relationship is obtained and the rate constants, K'', are estimated from those gradients. The values of K'' are shown with C_O, α and W in Table 6. The

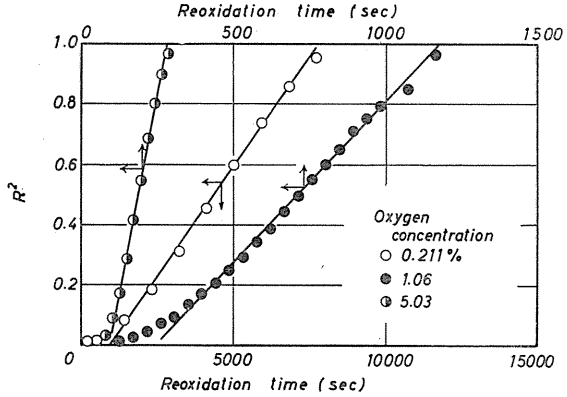

FIG. 25. Relation between R^2 and t for various oxygen concentration. (Reduction: 600°C)

TABLE 6. Estimated Values of K'' and $D_e/(\rho \cdot L^2)$ in Eq. (13)

Reduction temperature (°C)	$C^b_{O_2}$	α	W	K''	$D_e/(\rho \cdot L^2)$	Remarks
500	4.16×10^{-8}	0.539	0.2005	1.31×10^{-4}	10.3	Effect of $C^b_{O_2}$
〃	1.05×10^{-6}	0.515	0.1999	3.82×10^{-3}	11.9	
〃	4.16×10^{-6}	0.557	0.2017	1.16×10^{-2}	13.9	
600	4.16×10^{-8}	0.515	0.1999	1.43×10^{-4}	15.9	Effect of $C^b_{O_2}$
〃	2.09×10^{-7}	0.323	0.1991	1.08×10^{-3}	15.0	
〃	9.94×10^{-7}	0.298	0.1998	5.30×10^{-3}	14.3	
400	4.16×10^{-8}	0.480	0.2019	1.53×10^{-4}	15.8	Effect of reduction temp.
500	〃	0.539	0.2005	1.31×10^{-4}	15.2	
600	〃	0.515	0.1999	1.43×10^{-4}	16.0	
700	〃	0.144	0.2011	4.01×10^{-4}	12.5	
600	2.09×10^{-7}	0.370	0.0496	3.46×10^{-3}	54.5	Effect of W
〃	〃	0.380	0.2002	8.59×10^{-4}	14.0	
〃	〃	0.450	0.6027	2.56×10^{-4}	4.93	

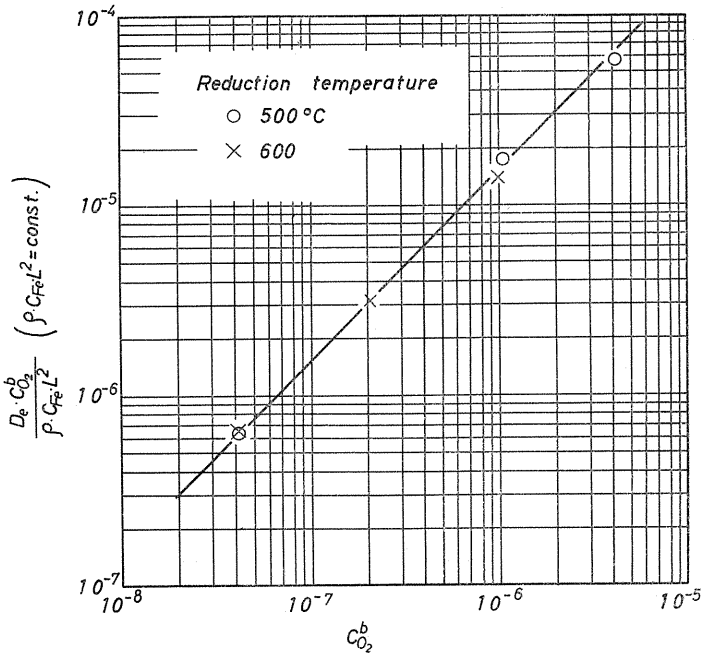

FIG. 26. Relation between $K''\alpha/2$ and oxygen concentration ($C^b{}_{O_2}$) in Eq. (13).

relations of $(K''\cdot\alpha)/2$ vs C_0 and K''/C_0 vs α are shown in log-log diagrams in Figs. 26 and 27, where linear relations are observed with gradients $+1$ and about -1, respectively.

Since D_e, ρ, C_{Fe} and L^2 are assumed to be independent of the reduction temperature, the gradient of $+1$ in Fig. 26 shows that the experimental results are well agreed with the theoretical equation.

If D_e, ρ and L^2 of reduced iron powders are assumed to be independent of the reduction temperature, the gradient of -1 in Fig. 27 also shows the agreement between the experimental results and the theoretical analysis. On the other hand, since the value of L can not be calculated exactly, the value of D_e is not estimated precisely. However, the value of $D_e/(\rho\cdot L^2)$ as shown in Table 6 is reasonable compared with gas diffusivity in the N_2–O_2 system at 400°C, 0.18/cm²/sec (273.2°K).

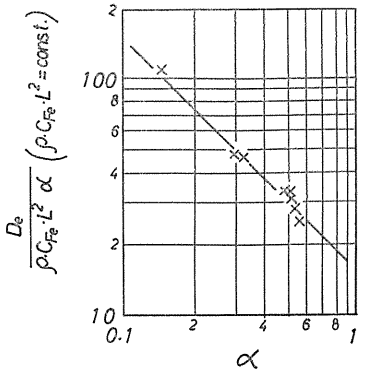

FIG. 27. Relation between $K''/C^b{}_{O_2}$ and α in Eq. (13).

2.5. Conclusions

The rate of reoxidation of the iron powders reduced from ferric oxide and Brazilian ore was studied. Following conclusions were clarified.

1) The reoxidation of reduced iron powders proceeds in two steps divided distinctly, that is, in the very rapid initial stage and the very slow later stage.

2) When the reduced iron powders are reoxidized, their specific surface areas change, showing some characteristic behaviors and depending on their physical properties. Generally, they show maximum values after several minutes of the biginning of reoxidation.

3) The iron oxide layer obtained at 400°C by reoxidation of the reduced iron powders shows magnetite and a small amount of hematite. Magnetite is obtained at the early stage of reoxidation and later hematite increases gradually.

4) The rate of reoxidation in the later stage is controlled by the oxidation process on the pore surface of reduced iron powders and represented by the logarithmic rate law.

5) The rate of reoxidation in the initial stage is controlled by the gas diffusion of oxygen through gas boundary layer and also reoxidized zone of iron powders packed.

Chapter III. Experimental Study of the Antiactivation of Reduced Pellets at Low Temperatures

3.1. Introduction

It is well known that the reduced pellets are easily reoxidized in air at room temperature. Especially, the pellets reduced at lower temperatures ignite in air.

Nevertheless, the reoxidation behaviors of reduced pellets have not yet been studied sufficiently. In order to prevent the ignition of sponge-iron powders reduced at lower temperatures, the treatment in the inert gas containing extremely low oxygen potential is known[41] to be effective. But the necessary oxygen potential and treating time for the antiactivation have not been made clear. Then the authors investigated the reoxidation behaviors of reduced pellets in order to know the necessary conditions for the antiactivation and also to clarify the mechanism of such antiactivation.

From the point of view of iron and steel industry, the pellets are generally reduced at higher temperatures, however, for the present study those pellets reduced at lower temperatures are rather significant.

3.2. Materials

In the present work, all the experiments were carried out with those hematite pellets which were prepared by balling of oxide particles and igniting for 6 hrs in air at 1300°C. The porosity of those pellets was 18 to 28 pct and pore surface areas were 11 to 13 sqm per gram.

3.3. Experimental apparatus and procedures

All the rate measurements were made with the same balance system shown in Fig. 1. The sensibility of the balance is 0.5 mg. The pellet was suspended from the balance in a reaction tube heated by an electric resistance furnace.

The reaction tube consisted of a 33 mm ID by 1000 mm long silica tube whose lower part was packed with alumina particles to preheat the reaction gas. The hot junction of Pt vs Pt 13 pct Rh thermocouple inserted from the bottom through a 6 mm silica protection tube was situated 5 mm below the sample.

The reduction and reoxidation of those pellets were carried out in series.

The pellet was weighed, placed in a Pt wire basket and suspended from the balance. While the pellet was heated to reduction temperature, the atmosphere in the reaction tube was purged with nitrogen. Hydrogen was then introduced and the weight loss was recorded at adequate time intervals. After the pellet was completely reduced to sponge iron, it was cooled to the reoxidation temperature in the same atmosphere and then the atmosphere in the reaction tube was purged with nitrogen. To remove oxygen as impurity in commercial grade nitrogen, so as to prevent the slightest reoxidation, nitrogen from the cylinder was flowed through the packed bed of copper chips which was reduced frequently by introducing hydrogen. Accordingly, any oxygen could not be detected by gas chromatgraph with high sensibility. Then, nitrogen containing some amounts of oxygen was introduced and the weight increase was recorded by the balance at adequate time intervals.

3.4. Experimental results

3.4.1. Reoxidation of reduced pellets under several oxygen potentials at room temperature

Those pellets reduced by hydrogen at 520°C were reoxidized with nitrogen containing various amounts of oxygen, from 29 ppm to 40 pct, at room temperature. The reoxidation curves were given in Figs. 28 and 29. As shown in these figures, if those reduced pellets are reoxidized under lower oxygen concentrations such as below 1 pct oxygen, the reoxidation does not proceed over 1.0 pct independent of oxygen potentials. On the other hand, under those oxygen potentials higher than 5 pct oxygen, the reoxidation proceeds with increasing oxygen potential. It is also observed that the reoxidation proceeds up to 1.0 pct more rapidly with increasing oxygen potential. The detailed description on the relationship between the reoxidation degrees and the oxygen potentials is referred to 3.4.5.

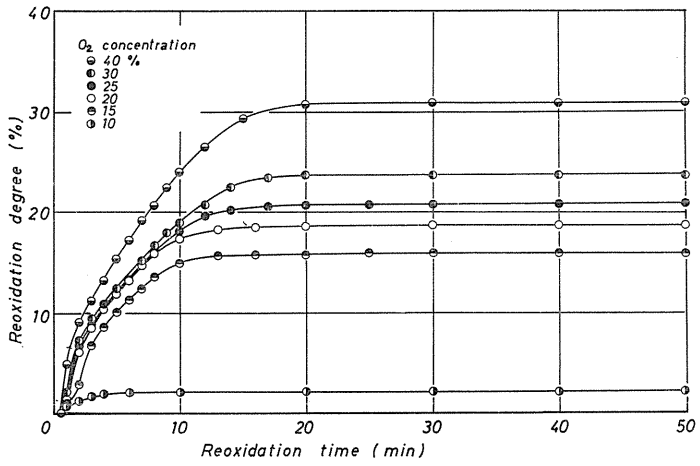

FIG. 28. Effect of the O_2 content on the reoxidation of reduced pellet. (O_2 content: over 10%, temperature: 25°C)

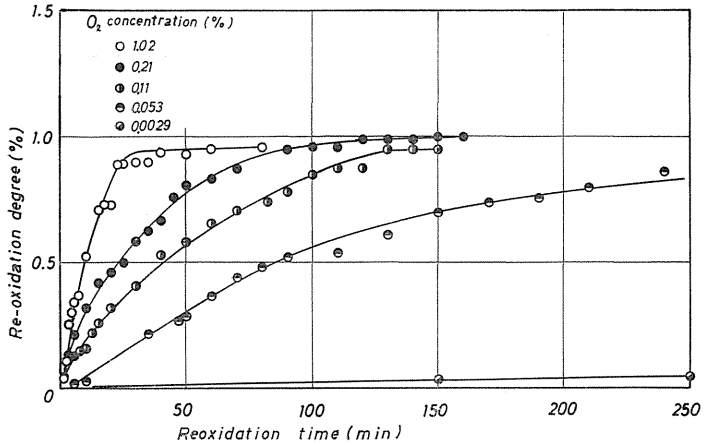

FIG. 29. Effect of the O_2 content on the reoxidation of reduced pellet. (O_2 content: below 1%, temperature: 25°C)

3.4.2. Heat evolved by reoxidation

Since the oxidation of metallic iron is exothermic and the reduced pellets have large reaction interface area, the temperature changes during the reoxidation must be taken into account to investigate the reoxidation behaviors.

When the raw pellet was prepared, the hot junction of Pt vs Pt 13 pct Rh thermocouple was settled so as to be placed at the center of the pellet. Then the raw pellet was heated in air at 1300°C for 6 hrs.

Those pellets were reduced by hydrogen at 500°C and then reoxidized in various oxygen potentials at room temperature.

The temperature change was recorded automatically during reoxidation. The results were shown in Fig. 30 where the diameters of pellets were written

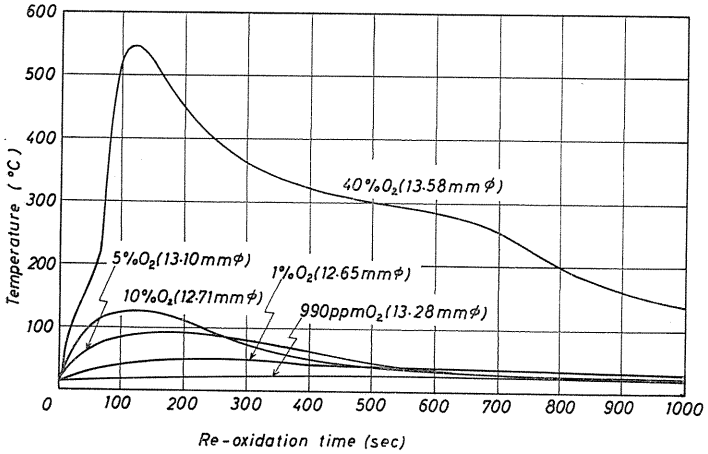

FIG. 30. Temperature changes of reduced pellets by reoxidation with N_2-O_2 gas mixture of various O_2 content. Figures in parentheses show diameters of pellets.

in parentheses.

The highest peak of the temperature curve during the reoxidation became higher and sharper, and the time to reach the peak became shorter with increasing oxygen potential. Below 1 pct oxygen, the temperature rises were relatively small.

3.4.3. Microscopic and X-ray analysis of reduced pellets reoxidized in various oxygen potentials at room temperature

In order to analyse the process of reoxidation, cross sections of the pellets reoxidized in various oxygen potentials were observed.

Macroscopic inspections of the fracture surfaces show that an light gray inner core is surrounded by a dark gray outer shell of oxide layer, when the oxygen potential is higher than 5 pct. A typical figure is shown in Photo 2.

The thickness of the macroscopic oxide layer increases with increasing oxygen potential above 5 pct oxygen. When the pellets were reoxidized in lower oxygen potential such as below 1 pct oxygen, the cross section was observed to be apparently uniform like the core shown in the Photo 2. The interface between the outer shell and inner core seems to be parallel to the surface. This fact suggests that the rate of oxidation of metallic iron on the pore surface is rapid compared with the rate of the oxygen diffusion in the reoxidized shell layer. Therefore, the reoxidation of reduced pellets might proceed topochemically.

Furthermore, microscopic observation shows that the macroscopic oxide shell layer consists of the thin oxide film on the pore surface and the metallic iron inside of this film. In the inner core, however, any microscopic oxide layer could not be observed. Those pellets reoxidized in the oxygen potential below 1 pct show no more microscopic oxide film. It was furthermore made clear that the visual colour of the macroscopic oxide shell might vary with the thickness of microscopic oxide films.

The typical microphotograph of the macroscopic oxide shell is shown in Photo 3.

The identification of metallic iron, wustite, magnetite and hematite in both parts was studied by X-ray diffraction, using iron turget. The results were listed

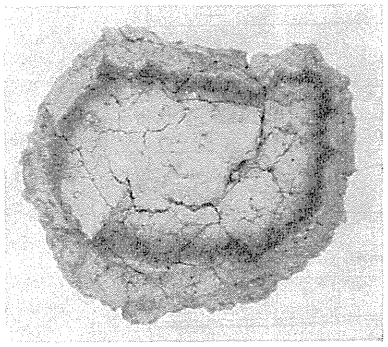

PHOTO 2. Cross sectional view of a reduced pellet, reduced by hydrogen at 520°C and re-oxidized by N_2-O_2 gas mixture at room temperature.

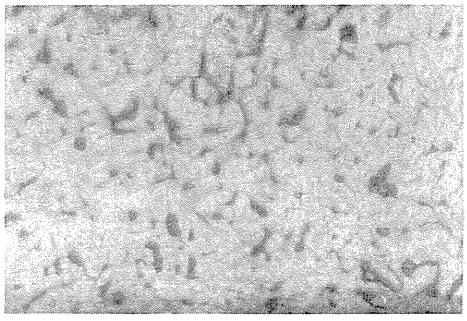

PHOTO 3. Microphotograph of the oxide layer of the re-oxidized (by 20% O_2-N_2 gas mixture) pellet which was reduced at 520°C, showing microscopic oxide layer and metallic iron.

TABLE 7. Results of X-ray Analyses of Reduced Pellets Reoxidized by Various Oxygen Concentrations

No.	Partial pressure of oxygen (atm)	Outside layer	Inner core
46	0.40	Fe, Fe_3O_4, Fe_2O_3	Fe
44	0.30	Fe, Fe_3O_4	Fe
42	0.25	Fe, Fe_3O_4	—
45	0.20	Fe, Fe_3O_4	Fe
41	0.10	Fe, Fe_3O_4	

in Table 7.

Hematite was detected only for the pellet reoxidized in the higher oxygen potential such as 40 pct oxygen and magnetite was seen for the pellet reoxidized in the oxygen potential higher than 5 pct. For those pellets reoxidized in the oxygen potential less than 1 pct and also for the inner cores reoxidized in the oxygen potential higher than 5 pct, nothing was observed except metallic iron.

3.4.4. Reoxidation of reduced pellets at 100°~300°C under lower oxygen potentials

As shown in 3.4.1, it is clear that if the reduced pellets are reoxidized to a definite degree under lower oxygen potential, they are not further reoxidized.

It is generally recognized that the rate of oxidation of metallic iron obeys logarithmic rate law at lower temperatures and parabolic rate law at higher temperatures. Concerning the transition temperature from logarithmic-to parabolic rate law, close agreement among earlier works was not necessarily obtained. However, it is clear that the logarithmic rate law is appliciable to the initial stage of the oxidation of iron at the temperature in the neighbourhood of A_1 transformation point of iron.

The authors have already shown in Chapter II that the logarithmic rate law is valid to the reoxidation of iron powders reduced by hydrogen.

According to the logarithmic rate law, the reoxidation proceeds very rapidly at first and its rate decreases after a definite period as if the further reoxidation seems to stop. Therefore, the present results that the reoxidation of reduced pellets seems to stop at a definite reoxidation degree may be resulted from the fact that

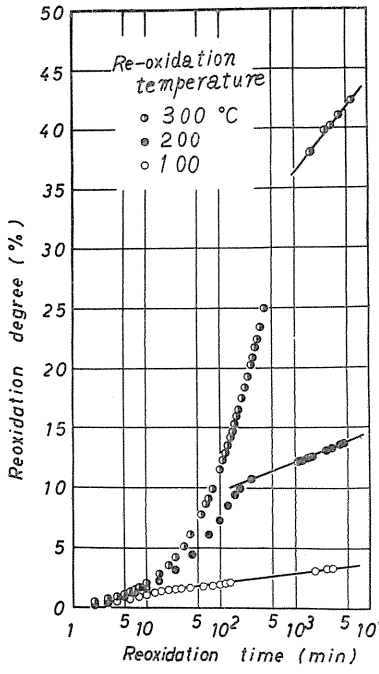

FIG. 31. Logarithmic plots of reoxidation curves of reduced pellets, reoxidized by N_2-O_2 gas mixture containing 1% O_2 at 100°~300°C.

the oxidation of metallic iron on the pore surface obeys the logarithmic rate law.

Then, in order to ascertain whether the logarithmic rate law might be valid to the reoxidation of reduced pellets or not, those pellets reduced at 520°C were reoxidized in the nitrogen containing 1 pct oxygen at 100°, 200°, and 300°C. Results were shown in Fig. 31 in the semi-log plots. Except the initial stage, it is clear that linear relationships may hold at each temperature. That is, the logarithmic rate law is applicable to each later stage. Now, it is defined that the initial reoxidation degree is that at which the logarithmic rate law begin to hold. In Fig. 32, the initial reoxidation degrees obtained from Fig. 31 are shown as Arrhenius-type plot. It shows that the initial reoxidation degree increases with increasing reoxidation temperature, especially above 100°C.

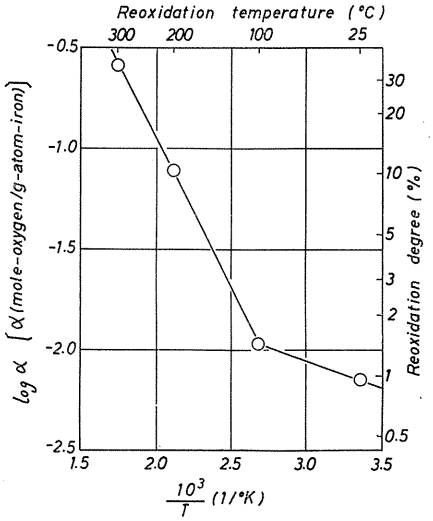

FIG. 32. Relation between reoxidation temperature and initial reoxidation degree of reduced pellet with gas containing 1%O_2.

3.4.5. Effect of the oxygen potential on the reoxidation degree

The relationship between the reoxidation degree and the oxygen potential in the range of 29 ppm to 40 pct oxygen is shown in Fig. 33. It is clear that although the reoxidation degree increases with oxygen concentration more than 5 pct oxygen, it is nearly constant below 1 pct oxygen independent of oxygen potential.

It is reasonable to consider that the reoxidation degree increases with increasing oxygen potential, due to the temperature rise of the pellet by the heat

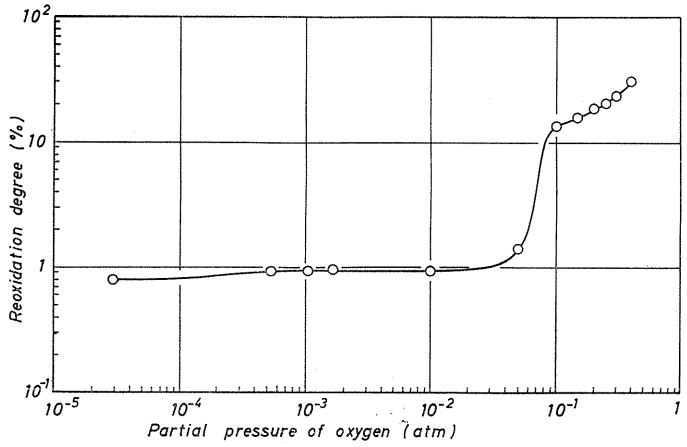

FIG. 33. Relation between the reoxidation degrees of reduced pellets (reduced at 520°C) and oxygen contents at room temperature.

of oxidation which accelerates reoxidation. If the oxygen potential is lower than 1 pct, the temperature rise is negligibly small and its effect on the reoxidation is also negligible. Therefore, it seems that the reoxidation degree is nearly constant below 1 pct oxygen at the room temperature. Even in the oxygen potential above 5 pct, if the temperature rise could be prevented, the reoxidation degree would not increase and show the similar values such as in the lower oxygen potential below 1 pct.

Considering that the inner structures of the reoxidized pellets in the oxygen potential below 1 pct are observed to be uniform microscopically, it seems that any part of the pellet should absorb the definite content of oxygen and show no more increase of reoxidation.

Since the reoxidation degree depends on the temperature rise during the reoxidation, the range of the oxygen potential where the reoxidation degree shows constant may also depend on the characteristics of heat conduction surrounding the sample such as the heat conductivity of gases.

It was also recognized that the pellet reoxidized in a lower oxygen potential was not further reoxidized even in a higher oxygen potential. Consequently, those pellets which have been slightly reoxidized in the oxygen potential below 1 pct are regarded as to be antiactivated.

3.4.6. Antiactivation of the pellets reduced at various temperatures

It is now quite clear that those pellets reduced at 520°C are antiactivated by reoxidizing in the low oxygen potential below 1 pct oxygen. Now, in order to ascertain the effects of reducing temperature on the reoxidation degree, those pellets reduced at the temperature in the range of 400° to 690°C were reoxidized in the lower oxygen potential of 0.1 pct oxygen. The results are shown in Fig. 34 which shows that the reoxidation degree decreases rapidly with increasing reduction temperature below 600°C. However, it decreases gradually above 600°C.

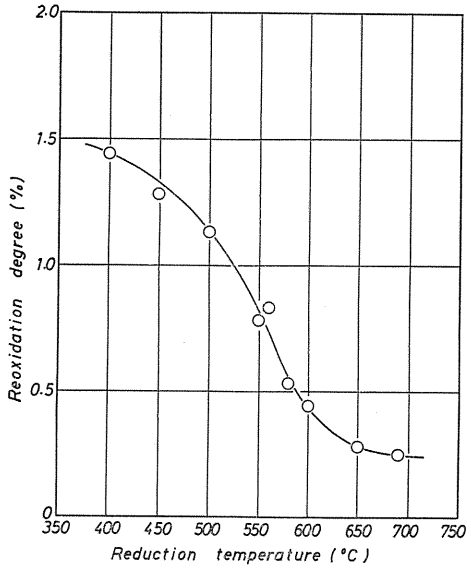

FIG. 34. Relation between the reoxidation degrees of reduced pellets and reduction temperatures.

3.4.7. Absorption amount of oxygen per unit surface area of the pellets reduced at various temperatures

In order to obtain the absorption amount of oxygen per unit surface area of reduced pellets, specific surface areas of those pellets reduced at various temperatures were measured by applying BET equation for adsorption isotherms of nitrogen at −195°C. The relationship between the specific surface areas and reduction temperatures are

shown in Fig. 35 which shows that the area decreases linearly with increasing reduction temperature. This is in good agreement with the previous works.

Now, if the composition of oxide layers could be analysed, the thickness of such layers would be calculated from the absorption amount of oxygen per unit area. However, this composition can not be determined by X-ray analysis as described in 3. 4. 3, and so the thickness of oxide layer was calculated by Eq. (14), assuming the oxide layer to be a simple iron oxide, that is, wustite, magneitie, or hematite, where their densities are 5.261 m^2/g, 5.136 m^2/g, and 5.73 m^2/g[4], respectively.

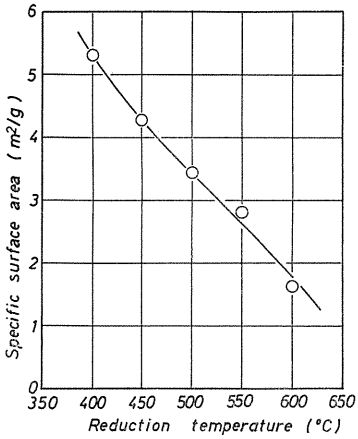

FIG. 35. Specific surface areas of reduced pellets reduced at various temperatures.

$$x\times 10^{-8}\times d_{\text{oxide}}\times\frac{yM_O}{M_{Fe}+yM_O}=\frac{\dfrac{F}{100}\times\dfrac{3M_O}{2M_{Fe}}}{S_w} \tag{14}$$

The results are shown in Fig. 36, which shows that the maximum thickness is obtained when the pellets are reduced at nearly 520°C independent of the kind of iron oxide. This maximum thickness is approximately 9 Å.

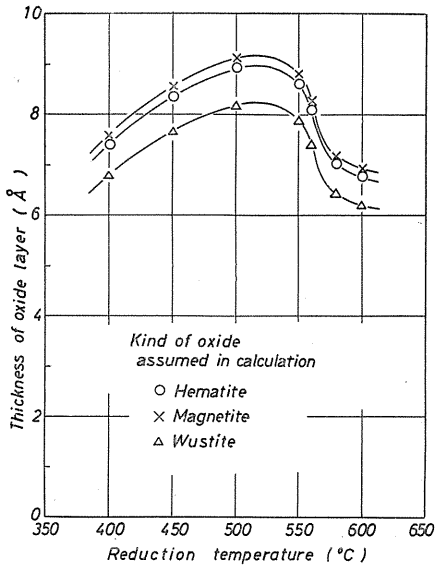

FIG. 36. Relations between the reduction temperatures of pellets and the calculated thicknesses of oxide layers of reduced pellets, reoxidized by gas containing 0.1% O_2 at room temperature.

3.5. Discussions

As described in 3.4.4, the logarithmic rate law is valid for the later

stage of the reoxidation of reduced pellets as the oxidation of metallic iron. Accordingly, if the oxygen supply is enough to the reaction interface, the reoxidation rate of the reduced pellet would also obey the same logarithmic rate law. Since the reduced pellet, however, is porous and has large specific surface area, oxygen molecule must diffuse inside of the pores from the gas bulk to reach the reaction interface. Furthermore, the reduced pellets are more strongly affected by the exothermic reaction of oxidation due to the large reaction interface. Those factors are different from the oxidation behavior of metallic iron. In the present work, the analyses of the reoxidation process were carried out when the remarkable temperature increase of the pellets was not observed by reoxidation in the low oxygen potential.

3.5.1. Reoxidation rate of metallic iron on the pore surface of reduced pellets

It is reasonable to consider that the oxidation rate law of metallic iron should be also applied to the reoxidation of metallic iron on the pore surface of the reduced pellet. In our previous works, it was shown that the logarithmic rate law was valid to the later stage of the reoxidation of reduced iron-powders, and furthermore it was also valid for the reduced pellets, as described in 3.4.4. It is generally accepted that the logarithmic rate law is valid to the oxidation of metallic iron at lower temperatures and also to the initial period of the oxidation at higher pemperatures.

According to the Mott's theory[36)37)], the logarithmic rate law can be applied to the oxidation of metals whose oxides are ion conductors and also electron insulators. Namely, the rate of oxidation is limitted by the rate of electron transfer. Electrons can penetrate through the oxide layer by tunnelling effect of quantum mechanics without going over the energy barrier. The probability of passing through is represented by $\exp(-x/x_0)$. The rate of growth of oxide layer is proportional to this probability and represented by Eq. (3).

$$dx/dt \propto \exp(-x/x_0) \tag{3}$$

Integrating Eq. (3), Eq. (4) is obtained

$$x = x_0 \log(t + t_0) - x_0 \log t_0 \tag{4}$$

when $t \gg t_0$, then Eq. (4) becomes

$$x = x_0 \log t - x_0 \log t_0 \tag{15}$$

Substituting Eq. (14) into Eq. (15), then

$$F = k \log t - k \log t_0 \tag{16}$$

$$k = S_w \times d_{\text{oxide}} \times \frac{yM_{\text{Fe}}}{M_{\text{Fe}} + yM_{\text{O}}} \times \frac{2}{3} \times 10^{-6} \times x_0 \tag{17}$$

Since the increase of the weight is approximately proportional to the thickness of the oxide layer, it is linearly proportional to logarithm of reoxidation time. The results in the present work satisfy the logarithmic rate law, as shown in 3.4.4.

It is suggested from the above theory that x_0 does not depend on the oxygen

potential, but depends on the temperature. Then, applying the results shown in Fig. 31, the values of k were estimated such as 0.363, 1.08, and 3.50 (−), respectively. They satisfied approximately Arrhenius-type relation, as shown in Fig. 37. The activation energy was estimated to be 4.8 kcal/mol which was slightly larger than 3 kcal/mol obtained in Chapter II for the reoxidation of reduced iron-powders, but remarkably less than 21.7 kcal/mol obtained for the oxidation of iron plate by Measor *et al.*[24]

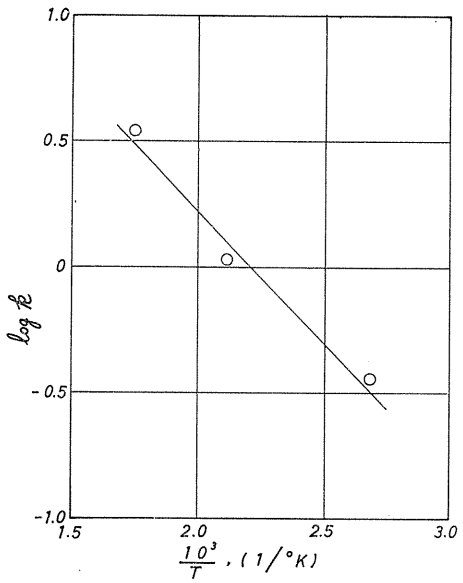

FIG. 37. Arrhenius plots of rate constants of reoxidation of reduced pellets as shown by logarithmic law.

3.5.2. *Reoxidation rate of reduced pellets*

As shown in 3.4.4, the reoxidation process of the reduced pellets is analysed by separating into the initial stage and the later one. Here, the present results show that the logarithmic rate law is valid to this later stage. It is generally recognized that this law is applicable to the oxidation of metallic iron at lower temperatures and the initial period of the oxidation of metallic iron at higher temperatures.

According to the logarithmic rate law, a metallic iron is rapidly oxidized to a definite reoxidation degree. In this case, the rate of reoxidation reaction of the metallic iron on the pore surface may be very rapid[23].

Therefore, it is concluded that the rate limitting step in the initial stage of the reoxidation of reduced pellets should not be the oxidation process on the pore surface but the gas diffusion process both in the boundary layers and in the reoxidized shell layers of reduced pellets, or the both processes of the gas diffusion and the reoxidation of the pore surface.

Furthermore, as described in 3.4.1, the initial rate of the reoxidation of reduced pellets increases with increasing oxygen potential. This fact also suggests that the initial stage of the reoxidation of reduced pellets is mainly controlled by the gas diffusion, for the rate constant, k, is independent of oxygen potential.

It is well known[42] that the gas-solid reaction proceeds topochemically when the rate of chemical reaction at the interface is remarkably rapid and the gas diffusion is rate controlling. This is confirmed by the macroscopic observation of cross sections of reduced pellets reoxidized in the oxygen potential above 5 pct.

If it is assumed that the reoxidation rate of the reduced pellet should be controlled by the gas diffusion in the gas boundary layer and the reoxidized shell layer, the rate equation can be written by Eq. (18), where the reoxidation model is shown in Fig. 38.

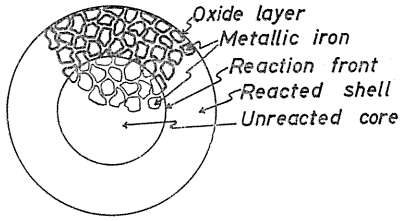

FIG. 38. Reoxidation model.

$$\frac{1}{D_e}\left[\frac{1}{2}\{1-(1-R)^{2/3}\}-\frac{1}{3}R\right]+\frac{R}{3k_f r_0}=\frac{C^b_{O_2}-C^r_{O_2}}{d_{iron}\cdot\alpha\cdot r_0^2}\cdot t \tag{18}$$

Since oxygen molecules react with iron atoms and disappear at the reaction interface, the number of molecules in gas phase decreases at the reaction interface. Hence, bulk flow occurs from bulk gas phase towards reaction interface.

The rate of transfer of oxygen with bulk fow and diffusion can be calculated by the following equation, assuming quasi-stationary state.

$$J^d_{O_2}+J^c_{O_2}=C_0\cdot\frac{D_e}{r_0}\cdot\frac{r}{r-r_0}\cdot\ln\frac{C_0}{C^{r_0}_{N_2}} \tag{19}$$

On the other hand, the rate of diffusion through shell layer is calculated by Eq. (20), neglecting bulk flow.

$$J^d_{O_2}=\frac{D_e}{r_0}\cdot\frac{r}{r-r_0}\cdot C^{r_0}_{O_2} \tag{20}$$

The ratio of the diffusion flux to total transfer flux is calculated by Eq. (21).

$$J^d_{O_2}/(J^d_{O_2}+J^c_{O_2})=\frac{C^{r_0}_{O_2}-C^r_{O_2}}{C_0\ln(C_0/C^{r_0}_{N_2})} \tag{21}$$

The relation in Eq. (21) shows that $J^d_{O_2}/(J^d_{O_2}+J^c_{O_2})$ may gradually approach to unity, namely $J^c_{O_2}$ may approach zero, when the concentration of oxygen $C^{r_0}_{O_2}$ approaches to zero. The transfer of oxygen by bulk flow may practically negligible at the oxygen potential less than 1 pct where the reoxidation rate is analysed in this study.

As mentioned above, it is observed that any part of the reduced pellet is reoxidized to a definite reoxidation degree.

Oxygen potential in equlibrium with iron and magnetite, 1.63×10^{-92} mol/cm^3, was substituted into $C^r_{O_2}$ which was negligible compared with $C^b_{O_2}$. Then, the rate equation is shown as follows.

$$\frac{1}{D_e}\left[\frac{1}{2}\{1-(1-R)^{2/3}\}-\frac{1}{3}R\right]+\frac{R}{3k_f r_0}=\frac{C^b_{O_2}}{d_{iron}\cdot\alpha\cdot r_0^2}\cdot t \tag{22}$$

Eq. (22) divided with R, Eq. (23) is obtained.

$$\frac{\frac{1}{2}\{1-(1-R)^{2/3}\}-\frac{1}{3}R}{R}=\frac{D_e\cdot C^b_{O_2}}{d_{iron}\cdot\alpha\cdot r_0^2}\cdot\frac{t}{R}-\frac{D_e}{3k_f r_0} \tag{23}$$

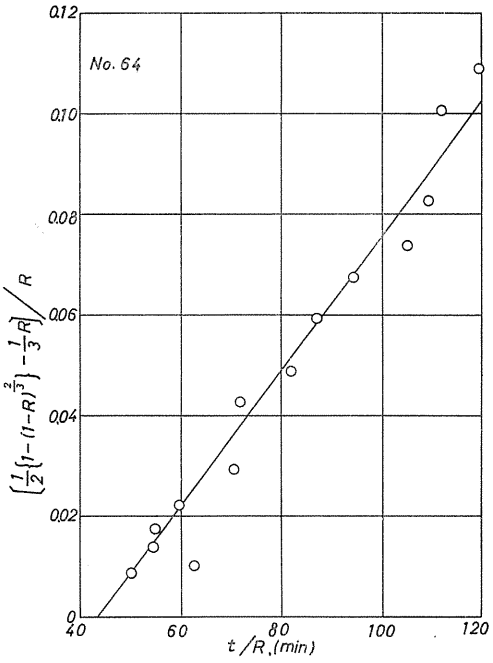

FIG. 39. Relation between $\left[\frac{1}{2}\{1-(1-R)^{2/3}\}-\frac{1}{3}R\right]/R$ and t/R in Eq. (23).

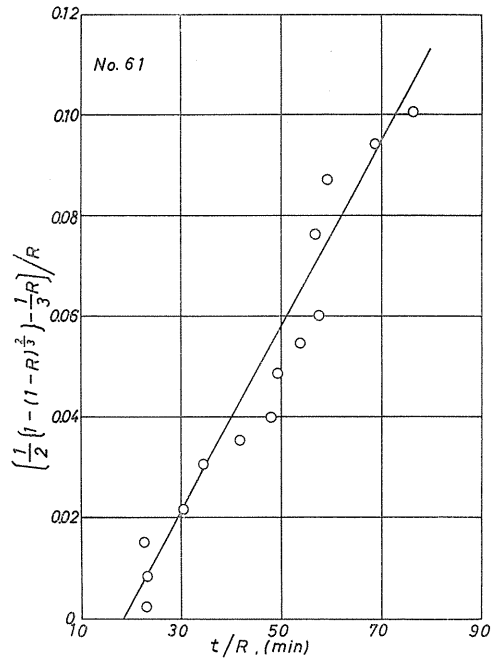

FIG. 40. Relation between $\left[\frac{1}{2}\{1-(1-R)^{2/3}\}-\frac{1}{3}R\right]/R$ and t/R in Eq. (23).

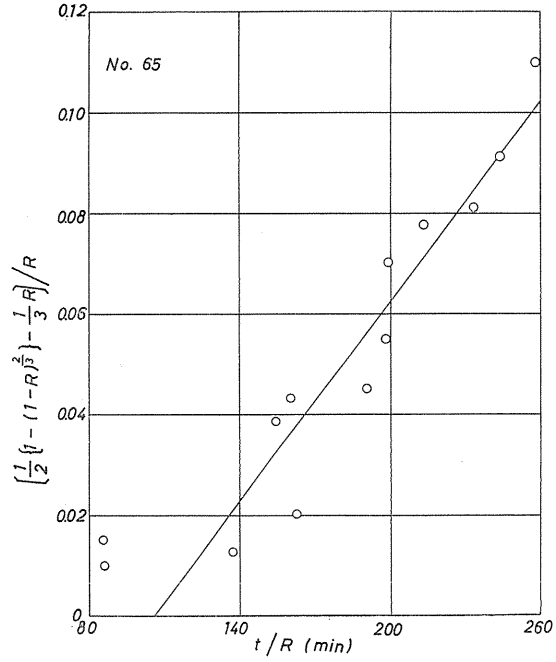

FIG. 41. Relation between $\left[\frac{1}{2}\{1-(1-R)^{2/3}\}-\frac{1}{3}R\right]/R$ and t/R in Eq. (23).

When the gas diffusion through either the reoxidized shell or the gas boundary layer, or through both of them may control the reoxidation rate, the relationship between $\left[\frac{1}{2}\{1-(1-R)^{2/3}\}-\frac{1}{3}R\right]/R$ in ordinate and t/R in abscissa should be linear. Effective diffusivity and mass transfer coefficient can be calculated by the slope and intersection in the plots of Eq. (23). The reoxidation curves in the present work satisfied the relation of Eq. (23) and shows the linear relationship, as shown in Figs. 39, 40, and 41.

The calculated values of D_e and k_f are listed in Table 8. It is clearly observed that D_e and k_f are approximately constant independent of the oxygen potential.

Applying the value of the gas diffusivity in the system N_2–O_2, $D_{N_2-O_2}=0.212$ cm^2/sec[43] at 25°C, the values of $D_e/D_{N_2-O_2}$ are also calculated and shown in Table 8.

Generally, in the reduction process of iron oxide pellet, the resistance of gas diffusion is significant at higher temperatures, while the resistance of chemical reaction is rather significant in lower temperatures[44]. Hence, at higher temperatures, D_e can be calculated by analysing the reduction curves. However, it is difficult at lower temperatures and so it has not yet been successfully calculated at lower temperatures. Therefore, it is necessary to apply another method. Recently, McKewan and coworker[45] measured the effective diffusivities in the H_2-H_2O system. In their experiment, the porous sample is sealed across an opening in an otherwise closed canister containing powders of iron and wustite. Thereafter, the canister in turn is suspended from a balance in the flow of hydrogen.

On the other hand, the present work gives the effective diffusivities by applying the same apparatus as for reduction. Nevertheless, since the reoxidation degrees become smaller as the reduction temperature rises, the balance with high sensibility must be used and the authors' method is not difficult to apply when the pellet is reduced at higher temperatures.

Concerning the value of k_f, it can be also calculated from the correlations

TABLE 8. Experimental Results of Effective Diffusion Coefficient D_e and Mass Transfer Coefficient k_f of Reoxidation of Reduced Pellets

No.	$C^b_{O_2}\left(\frac{mol}{cm^3}\right)$	$\alpha\left(\frac{mol\text{-}oxygen}{g\text{-}atom\text{-}iron}\right)$	r_0(cm)	$d_{iron}\left(\frac{g\text{-}atom}{cm^3}\right)$	$D_e\left(\frac{cm^2}{sec}\right)$
62	4.18×10^{-7}	7.09×10^{-3}	0.662	5.16×10^{-2}	0.054
61	8.61×10^{-8}	7.15×10^{-3}	0.620	5.05×10^{-2}	0.079
64	4.51×10^{-8}	8.48×10^{-3}	0.633	4.74×10^{-2}	0.079
65	2.17×10^{-8}	6.93×10^{-3}	0.608	5.04×10^{-2}	0.065
67	1.19×10^{-9}	5.92×10^{-3}	0.576	5.08×10^{-2}	0.067

No.	$D_e/D_{N_2\text{-}O_2}\left(\frac{cm}{sec}\right)$	$k_f^{expt}\left(\frac{cm}{sec}\right)$	k_f^{calc}(R.M.)$\left(\frac{cm}{sec}\right)$	k_f^{calc}(S.T.)$\left(\frac{cm}{sec}\right)$
62	0.25	0.26	0.809	0.728
61	0.37	0.81	0.847	0.760
64	0.37	0.72	0.835	0.749
65	0.31	0.51	0.843	0.756
67	0.32	1.10	0.892	0.803

of dimensionless numbers, that is, Ranz-Marshall relation Eq. (24) and Steinberger-Treyball relation Eq. (25).

$$Sh = 2.0 + 0.6\ Re^{1/2} \cdot Sc^{3/1} \tag{24}$$

$$Sh = 2.0 + 0.343\ Re^{0.62} \cdot Sc^{0.41} \tag{25}$$

The results are listed together in Table 8.

3.6. Conclusions

The pellets reduced at lower temperatures are ignited if they are exposed to atmosphere, as the sponge iron powders reduced at the similar condition. In order to reveal the reoxidation phenomena and to prevent the ignition, the reoxidation of reduced pellets was investigated over the oxygen potential range of 29 ppm to 40 pct at room temperature.

The reoxidation behaviors of the reduced pellets are different from the oxidation of metallic iron. Namely, the oxygen molecules must diffuse through the pore to reach the pore surface where the reaction occurs and also the reoxidation is strongly influenced by the temperature increase due to the heat of oxidation itself, as the specific reaction interface is larger than the metallic iron plate. In the present work, the analysis of the reoxidation rate was carried out on the former case and the following conclusions were obtained.

1) If the reduced pellets are reoxidized to the definite reoxidation degrees further reoxidation does not preceed even in the higher oxygen potentials.

2) While the final reoxidation degree increases with increasing oxygen potential when the potential is higher than 5 pct oxygen, it shows, however, constant values independent of the oxygen potential which is lower than 1 pct. The reoxidation degree which is obtained in lower oxygen potential may be determined by the characteristics of the reduced pellets.

3) The results that the reoxidation degree increases with increasing oxygen potential above 5 pct, could be interpretted by the temperature rise due to the heat of reaction which promotes the reoxidation, especially above 100°C. The reoxidation degree would show a definite value if the temperature rise could be prevented by the sufficiently rapid cooling.

4) The rate of the reoxidation are controlled by the gas diffusion through the gas boundary layer and the reoxidized shell layer. Therefore, the time required for the antiactivation of the reduced pellets can be calculated from the gas diffusion controlling model.

5) The results that the reoxidation seems to stop after a slight reoxidation up to a definite degree in the lower oxygen potential such as below 1 pct would be interpretted by the logarithmic rate law which is valid for the rate of the reoxidation.

6) The macroscopic oxide shell layer is formed when the pellets are reoxidized in the oxygen potential above 5 pct. This oxide shell layer are composed of the microscopic oxide film and the metallic iron remained beneath the film. The macroscopic inner cores are apparently composed of the metallic iron alone, so far as by X-ray and microscopic examinations, as observed on the pellets reoxidized below 1 pct oxygen.

Summary

In the present study, the reoxidation behaviors of the iron reduced from ferric oxide and various kinds of iron ores were clarified.

The reoxidation behavior of the reduced iron was regarded as the process composed of the two stages—the initial stage which shows a very rapid oxidation and the later which shows a very slow oxidation. The analysis of the results on the reoxidation process shows that the rate of reoxidation in the initial stage is controlled by the gas diffusion in the gaseous boundary layer and also reduced iron layer, on the other hand, in the later stage it is controlled by a transport inside of the solid.

It is also pointed out that the temperature rise resulted from the heat of oxidation accelerates the reoxidation of the sample. Therefore, it is possible to lower the reoxidation degree, if the oxygen potential of the gas mixtures is controlled as possible as low. The present results on the reduced iron pellets show that the reoxidation degree under the lower oxygen potential such as less than 1% oxygen shows a low value independent of the oxygen potential. On the contrary, if the oxygen in the gas mixture increases more than 5%, the reoxidation degree increases as increasing the oxygen potential. It is also noteworthy that those reduced pellets slightly oxidized under lower oxygen potential less than 1 pct were not oxidized in the air; namely such reduced pellets were aparently antiactivated. This results are considerably valuable for the industrial utilization of reduced pellets. The reason of the antiactivation is regarded as the slow reoxidation rate obeyed to the logarithmic rate law in the room temperature.

The effects of the kind of iron ores and the temperature of reduction on the reoxidation behavior are also the main subject of this study. It is observed that the reduced iron powders from those ores which show good reducibility are reoxidized remarkably, such as limonite and hematite. Those from magnetite show less reoxidation degree.

Such reoxidation behaviors are probably resulted from the difference of the physical properties of original ores, since the values of their specific surface area are approximately proportional to the reoxidation degrees. The reoxidation degree at 400°C gives the maximum value when the iron ores are reduced at about 600°C, while it gives generally higher values as decreasing the reduction temperature. This characteristic behaviors are probably controlled by such factors as the specific surface area and the pore distribution of the reduced iron powders.

Nomencrature

A : area of reaction interface (cm^2)
C : gas concentration ($mol \cdot cm^{-3}$)
C_0 : total concentration of gas ($mol \cdot cm^{-3}$)
C_{Fe} : weight ratio of metallic iron (−)
D_e : effective diffusivity ($cm^2 \cdot sec^{-1}$)
$D_{N_2-O_2}$: gas diffusivity in the system N_2–O_2 ($cm^2 \cdot sec^{-1}$)
d_{iron} : apparent density of iron in the reduced pellet ($g\text{-}atom \cdot cm^{-3}$)
d_{oxide} : apparent density of iron oxide in the reoxidized pellet ($g \cdot cm^{-3}$)

F : reoxidation degree (pct)
F_0 : initial value of reoxidation degree (pct)
G_1 : gas reactant
J, J_3, J_4, J_5: flux of mass transfer ($mol \cdot cm^{-2} \cdot sec^{-1}$)
K : equlibrium constant of the gaseous reduction of iron oxide (−)
K', K'': apparent rate constant
k : rate constant ($g \cdot cm^{-2}$)
k' : rate constant of cubic-, linear-, logarithmic-, and parabolic rate law
k_f : mass transfer coefficient in the gas film ($cm \cdot sec^{-1}$)
L : height of packed bed (cm)
M_O : atomic weight of oxygen
M_{Fe} : atomic weight of iron
Δm : weight increase by reoxidation (g)
Δm_0 : initial value of Δm (g)
R : ratio of the reoxidation degree at t to the initial reoxidation degree (−)
r : radius of unreacted core (cm)
r_0 : radius of pellet (cm)
Re : Reynolds number (−)
S_1 : solid reactant
S_2 : solid product
Sc : Schmidt number (−)
Sh : Sherwood number (−)
S_w : specific surface area ($cm^2 \cdot g\text{-iron}^{-1}$)
T : absolute temperature (°K)
t : reoxidation time (sec)
t_0 : characteristic time (sec)
v : flow rate ($cm^3 \cdot cm^{-2} \cdot sec^{-1}$)
w : weigh of sample (g)
x : thickness of oxide layer (cm)
x_0 : characteristic length (cm)
y : number of oxygen atoms combined with one atom of iron
Z : distance from the surface of packed bed (cm)
α : initial reoxidation degree expressed in ($mol\text{-oxygen} \cdot g\text{-atom-iron}^{-1}$)
ρ : apparent density ($g \cdot cm^{-3}$) or variable showing the distance from the center of pellet (cm)

Subscripts and superscripts

1 : reactive gas (oxygen)
2 : inert gas (nitrogen)
b : bulk
c : bulk flow
d : diffusive flow
e : equlibrium
expt : experimental value
calc : theoretically calculated value

Appendix

Jost[46] has derived the rate equation of bulk flow and diffusion in the gas-solid reaction.

Here, we derived those of both bulk flow and diffusion in reaction (26) under the boundary conditions of reoxidation.

$$S_1 + \nu G_1 \rightarrow S_2 \tag{26}$$

Now, consider the system in which gas molecules reach the reaction interface and react with solid reactant as described by reaction (26).

Reaction model is shown in Fig. 42. Since gas molecules consumes at the reaction interface, gaseous reactant are transported to the interface by both diffusion and bulk flow. The flow rates are derived assuming the quasi-stationary state.

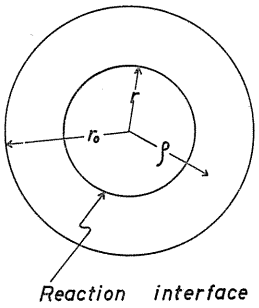

FIG. 42. A schematic model of reaction front.

The bulk flow in the direction of $+\rho$ is shown by Eq. (27).

$$v\rho^2 = v_0 r_0^2, \quad v = v_0 \cdot \frac{r_0^2}{\rho^2} \tag{27}$$

The diffusion rate is represented by Eq. (28),

$$J_1^d = -D_e \frac{\partial C_1}{\partial \rho}, \; J_2^d = -D_e \frac{\partial C_2}{\partial \rho} = D_e \cdot \frac{\partial C_1}{\partial \rho} \tag{28}$$

and the flow rate due to the bulk flow is also shown by Eq. (29).

$$J_1^c = C_1 v = C_1 v_0 \frac{r_0^2}{\rho^2}, \; J_2^c = C_2 v = C_2 v_0 \frac{r_0^2}{\rho^2} \tag{29}$$

Therefore, the total flow is shown by Eq. (30)

$$J_1 = -D_e \cdot \frac{\partial C_1}{\partial \rho} + C_1 v_0 \frac{r_0^2}{\rho^2} \tag{30 a}$$

$$J_2 = D_e \cdot \frac{\partial C_1}{\partial \rho} + C_2 v_0 \frac{r_0^2}{\rho^2} \tag{30 b}$$

$$J_1 + J_2 = (C_1 + C_2) \cdot v_0 \cdot \frac{r_0^2}{\rho^2} = C_0 \cdot v_0 \cdot \frac{r_0^2}{\rho^2} \tag{30 c}$$

Taking the mass balance within the shell layer of radius ρ and thickness $d\rho$, the time-dependent diffusion equation for component 1 is

$$\frac{\partial C_1}{\partial t} = -\operatorname{div}(J_1) = D_e\left[\frac{\partial^2 C_1}{\partial \rho^2}+\frac{2}{\rho}\cdot\frac{\partial C_1}{\partial \rho}\right]-\frac{v_0 r_0^2}{\rho^2}\cdot\frac{\partial C_1}{\partial \rho} = 0 \tag{31}$$

Here, $\partial C_1/\partial t$ is equal to zero for a quasi-stationary state.

In the case C_1 depends on ρ alone and Eq. (32) is obtained instead of Eq. (31)

$$\rho^2 C_1'' + C_1'(2\rho - \beta) = 0 \tag{32}$$

where dashes denote differentiation with respect to ρ and the length β is shown by Eq. (33).

$$\beta = v_0 r_0^2/D_e \tag{33}$$

Eq. (32) is to be solved under the following boundary conditions:

$$(J_2)_r = 0 \quad \text{at } \rho = r \tag{34 a}$$

$$C_1 = 0 \quad \text{at } \rho = r \tag{34 b}$$

$$(J_1)_{r_0} = (J_1)_r\cdot\frac{r^2}{r_0^2} \tag{34 c}$$

Substituting Eq. (30 b) into Eq. (34 a), then

$$D_e\left(\frac{\partial C_1}{\partial \rho}\right)_r = -C_2^r\cdot v_0\cdot\frac{r_0^2}{r^2} \tag{35}$$

and substituting Eq. (30 a) into Eq. (34 c) and using Eq. (34 b), Eq. (36) is obtained.

$$-D_e\left(\frac{\partial C_1}{\partial \rho}\right)_{r_0} + C_1^{r_0}\cdot v_0 = -D_e\left(\frac{\partial C_1}{\partial \rho}\right)_r\cdot\frac{r^2}{r_0^2} \tag{36}$$

Putting C_1' in Eq. (32) equal to ξ, then

$$\frac{d\ln\xi}{d\rho} = \frac{\beta - 2\rho}{\rho^2} \tag{37}$$

and integrating between r_0 and r, Eq. (38) is obtained.

$$\ln\frac{\xi}{\xi_0} = \frac{\beta}{r_0}-\frac{\beta}{\rho}-2\ln\frac{\rho}{r_0} \tag{38}$$

$$\frac{\xi}{\xi_0} = \left(\frac{r_0^2}{\rho}\right)^2\exp\left(\frac{\beta}{r_0}\right)\exp\left(-\frac{\beta}{\rho}\right) \tag{38 a}$$

Substituting Eq. (33) into Eq. (38 a), then

$$\left(\frac{\partial C_1}{\partial \rho}\right)_r = \left(\frac{\partial C_1}{\partial \rho}\right)_{r_0}\cdot\frac{r_0^2}{r^2}\exp\left(\frac{v_0 r_0}{D_e}\right)\exp\left(-\frac{v_0 r_0^2}{rD_e}\right) \tag{39}$$

From Eq. (35) and Eq. (36), the following Eq. (40) is obtained.

$$D_e\left(\frac{\partial C_1}{\partial \rho}\right)_{r_0} = C_1^{r_0}\cdot v_0 - C_2^{r}\cdot v_0 = -C_2^{r_0}\cdot v_0 \tag{40}$$

From Eq. (36) and Eq. (39), Eq. (41) is obtained.

$$C_1^{r_0}\cdot v_0 = D_e\left(\frac{\partial C_1}{\partial \rho}\right)\left[1-\exp\left(\frac{v_0 r_0}{D_e}\right)\exp\left(-\frac{v_0 r_0^2}{rD_e}\right)\right] \tag{41}$$

Substituting Eq. (41) into Eq. (40), the following Eq. (42) is obtained

$$C_1^{r_0}\cdot v_0 = -C_2^{r_0}\cdot v_0\left[1-\exp\left(\frac{v_0 r_0}{D_e}\right)\exp\left(-\frac{v_0\cdot r_0^2}{rD_e}\right)\right] \tag{42}$$

Solving Eq. (42) for the exponentials and taking logarithms, Eq. (43) and Eq. (44) are obtained finally.

$$\frac{v_0 r_0}{D_e} - \frac{v_0 r_0^2}{rD_e} = \ln\frac{C_1^{r_0}+C_2^{r_0}}{C_2^{r_0}} \tag{43}$$

$$v_0 = \frac{D_e}{r_0}\cdot\frac{r}{r-r_0}\cdot\ln\frac{C_1^{r_0}+C_2^{r_0}}{C_2^{r_0}} \tag{44}$$

Changing ρ into r_0 and substituting Eq. (40) into Eq. (44), Eq. (45) is obtained

$$J_1 = -D_e\cdot\left(\frac{\partial C_1}{\partial \rho}\right)_{r_0} + C_1^{r_0}\cdot v_0 = (C_1^{r_0}+C_2^{r_0})\cdot v_0 \tag{45}$$

and substituting Eq. (44) into Eq. (45), we have also

$$J_1 = C_0\cdot\frac{D_e}{r_0}\cdot\frac{r}{r-r_0}\cdot\ln\frac{C_0}{C_2^{r_0}} \tag{46}$$

Next, the flow rate is to be calculated by the diffusion alone, neglecting bulk flow. Eq. (47) is obtained from Eq. (28).

$$J_1^d = \frac{D_e}{r_0}\cdot\frac{r}{r-r_0}\cdot(C_1^r - C_1^{r_0}) \tag{47}$$

Substituting Eq. (34 b) into Eq. (47), Eq. (48) is obtained.

$$J_1^d = \frac{D_e}{r_0}\cdot\frac{r}{r-r_0}\cdot C_1^{r_0} \tag{48}$$

References

1) L. von Bogdancy, H. P. Schultz, B. Würzner, and I. N. Stranski: Arch. Eisenhüttenw., **34** (1963), p. 401.
2) S. Kondo, Y. Hara, M. Sugata and M. Tutiya: Tetsu-to-Hagané, **53** (1967), p. 724.
3) A. Ōkura and Y. Matsushita: Tetsu-to-Hagané, **51** (1965), p. 11.
4) O. Kubaschewski and B. E. Hopkins: "Oxidation of metals and alloys" (1962), (Butterworths and Co. Ltd., London).
5) S. Kasaoka and Y. Murata: Kogyo Kagaku Zasshi (J. Chem. Soc. Japan, Ind. Chem. Sec.), **64** (1961), p. 978.
6) *ibid*, **64** (1961), p. 986.

7) K. Fischbeck and F. Salzer: Metallwirtschaft, **14** (1935), p. 733 and 753.
8) B. J. Nelson: J. Chem. Phys., **6** (1938), p. 606.
9) G. Jackson and A. G. Quarrell: Iron Steel Inst. Spec. Rep., **24** (1939), p. 65.
10) M. H. Davies, M. T. Simnad, and C. E. Birchenal: J. Metals, **3** (1951), p. 889, **5** (1953), p. 1250.
11) L. Himmel, R. F. Mehl, and C. E. Birchenal: *ibid.*, **4** (1952), p. 147.
12) K. Hauffe: Metalloberfläche (A), **8** (1954), p. 97.
13) J. K. Stanley, J. von Hoene, and R. T. Huntoon: Trans. Amer. Soc. Metals, **43** (1951), p. 426.
14) W. H. J. Vernon, E. A. Calnan, C. J. B. Clews and T. J. Nurse: Proc. Roy. Soc. **A 216** (1953), p. 375.
15) Pfeiffer and C. Laubmeyer: Z. Elektrochem., **59** (1955), p. 379.
16) D. E. Davies, U. R. Evans and J. N. Agar: Proc. Roy. Soc., **225** (1954), p. 443.
17) J. Paidassi: Acta Met., **6** (1958), p. 184.
18) N. G. Schmahl, H. Baumann and H. Schenck: Arch. Eisenhüttenw., **29** (1958), p. 41 and p. 147.
19) C. Wagner: Z. Physik Chem., **21** (1933), p. 25.
20) W. D. Kingery, D. C. Hill and R. R. Nelson: A. Amer. Ceram. Soc., **43** (1960), p. 473.
21) L. von Bogdandy and H. J. Engell: "Die Reduktion der Eisenerze" (1967), p. 20. (Springer-Verlag, Berlin).
22) L. Pauling: "The nature of the Chemical Bond, (1940), (Cornell Uni. Press, Now York).
23) K. Fueki and S. Kurihara: Bull. Japan Inst. Metals, **8** (1969), p. 20.
24) J. C. Measor and K. K. Afzulpurkar: Phil. Mag., **107** (1964), p. 817.
25) L. B. Pfeil: J. Iron Steel Inst., **123** (1931), p. 237.
26) A. B. Winterbottom: *ibid.*, **165** (1950), p. 9.
27) E. A. Gulbransen: Trans. Electrochem. Soc., **81** (1942), p. 327.
28) G. Pfeifferkorn: Z. Metallk., **46** (1955), p. 204.
29) V. R. Evans: Trans. Electrochem. Soc., **91** (1947), p. 547.
30) N. B. Pilling and R. E. Bedworth: J. Inst. Metals., **29** (1923), p. 529.
31) K. Heindlhofer and B. M. Larsen: Trans. Amer. Soc. Steel Treat., **21** (1933), p. 865.
32) A. Portevin, E. Pretet and H. Jolivet: Rev. Metall., **31** (1934), p. 101, 186, 319.
33) J. Paidassi: Ing. quim., **10** (1951), p. 5.
34) O. Kubaschewski and D. M. Brascher: Trans. Faraday Soc., **55** (1959), p. 1200.
35) J. Moreau and M. Cagnet: Rev. Metall., **55** (1958), p. 1091.
36) N. F. Mott: Trans. Farad. Soc., **36** (1940), p. 472.
37) N. Cabrera and N. F. Mott: Rep. Progr. in Physics, **12** (1949), p. 163.
38) H. H. Uhlig: Acta Met., **4** (1956), p. 541.
39) H. H. Uhlig, J. Pickett and J. Macnairn: *ibid.*, **7** (1959), p. 111.
40) R. Tylecote: J. Inst. Metals, **78** (1950), p. 327.
41) S. Kondo, R. Matsumoto and K. Wada: Tetsu-to-Hagané, **50** (1964), p. 1648.
42) M. Ishida and C. Y. Wen: AIChE, **14** (1968), p. 311.
43) Kagaku Kogaku Kyokai: "Handbook of Chem. Eng." (1968), p. 60 (Maruzen Co.).
44) A. Moriyama, J. Yagi and I. Muchi: J. Japan Inst. Metals, **29** (1965), p. 528.
45) R. G. Olsson and W. M. McKewan: Met. Trans., **1** (1970), p. 1507.
46) W. Jost: Chem. Eng. Sci., **2** (1953), p. 199.